ORIGINAL ARTICLE

GR/Ahi1 regulates WDR68-DYRK1A binding and mediates cognitive impairment in prenatally stressed offspring

Bin Wei[1] · Haixia Shi[2] · Xi Yu[1] · Yajun Shi[1] · Hongtao Zeng[1] · Yan Zhao[1] · Zejun Zhao[1] · Yueyang Song[1] · Miao Sun[1] · Bin Wang[1]

Abstract

Accumulating research shows that prenatal exposure to maternal stress increases the risk of behavioral and mental health problems for offspring later in life. However, how prenatal stress affects offspring behavior remains unknown. Here, we found that prenatal stress (PNS) leads to reduced Ahi1, decreased synaptic plasticity and cognitive impairment in offspring. Mechanistically, Ahi1 and GR stabilize each other, inhibit GR nuclear translocation, promote Ahi1 and WDR68 binding, and inhibit DYRK1A and WDR68 binding. When Ahi1 deletion or prenatal stress leads to hyperactivity of the HPA axis, it promotes the release of GC, leading to GR nuclear translocation and Ahi1 degradation, which further inhibits the binding of Ahi1 and WDR68, and promotes the binding of DYRK1A and WDR68, leading to elevated DYRK1A, reduced synaptic plasticity, and cognitive impairment. Interestingly, we identified RU486, an antagonist of GR, which increased Ahi1/GR levels and improved cognitive impairment and synaptic plasticity in PNS offspring. Our study contributes to understanding the signaling mechanisms of prenatal stress-mediated cognitive impairment in offspring.

Keywords Prenatal stress · Offspring · Cognitive impairment · Risk factor · Competition

Abbreviations

AHI1	Abelson helper integration site 1
PNS	Prenatal stress
FOAD	Fetal Origins Adult Disease
HPA	Hypothalamic–pituitary–adrenal
WDR68	WD40 repeat sequence 68
DYRK1A	Dual-specificity tyrosine phosphorylation regulated kinase 1A
KO	Knockout
MDD	Major depressive disorder
Hap1	Huntingtin-associated protein 1
AD	Alzheimer's disease
MWM	Morris water maze
NOR	Novel object recognition
LTP	Long-term potentiation
PPF	Paired-pulse facilitation

Bin Wei and Haixia Shi contributed equally to this work.

✉ Miao Sun
  miaosunsuda@163.com

✉ Bin Wang
  binwang2233@suda.edu.cn

1 Institute for Fetology, The First Affiliated Hospital of Soochow University, Suzhou 215006, China

2 Institute of Neuroscience, Soochow University, Suzhou 215123, China

Introduction

The Fetal Origins Adult Disease (FOAD) hypothesis was proposed by Professor David Barker in the late 1980s and focuses on the relationship between chronic adult diseases and various adverse stimuli during early fetal development [1]. Early life represents a window of phenotypic plasticity that is critical to later adult health, and multiple prenatal stressors (such as hypoxia, maternal smoking, administration of excess glucocorticoids) can lead to a series of changes in fetal development that ultimately increase the risk of chronic disease in offspring, including cardiovascular disease, type 2 diabetes and many neurological disorders such as cognitive impairment, anxiety and depression [2–5]. The most widely studied system in early life that is susceptible to environmental programming is the hypothalamic–pituitary–adrenal (HPA) axis [6]. Acute or short-term activation of the HPA axis facilitates responses to stimuli, while chronic or long-term activation leads to harmful effects [7, 8]. Prenatal stress

induced excess glucocorticoids (GC) cross the placenta into the fetus, leading to decreased expression of glucocorticoid receptors (GR) in the fetal brain, and decreased expression of GR may lead to decreased negative feedback of glucocorticoid control, thereby increasing HPA axis activity in offspring [7, 9–11]. The hippocampus plays an important role in response inhibition, memory, spatial cognition, and maintenance of homeostasis of the HPA axis, and contains high levels of GR [12, 13], which makes the hippocampus more susceptible to prenatal stress than most other brain regions, and makes it a common candidate for investigating brain correlates of prenatal stress [14, 15]. Studies have shown that prenatal stress alters neuronal and synaptic development, affects the density and complexity of dendritic spines in the hippocampus or prefrontal cortex of the offspring and impairs cognition [16–21]. Although the fetal origins of cognitive impairment have been frequently discussed, the underlying molecular mechanisms remain uncertain.

The *AHI1* gene plays a critical role in brain development, and mutations in *AHI1* can lead to Joubert syndrome, a rare autosomal recessive disorder characterized by abnormal brain development and cognitive impairment [22]. Our previous study found that Ahi1 knockout (KO, Ahi1$^{-/-}$) mice exhibit depressive-like behaviors [23–26], and the expression of AHI1 in peripheral blood monocytes and macrophages is reduced in patients with major depressive disorder (MDD) [27]. Ahi1 and GR are mutually stabilized in the cytoplasm, and stress-induced extensive GR nuclear translocation reduces GR binding to cytoplasmic Ahi1, leading to Ahi1 ubiquitination and degradation. Conversely, reduction of Ahi1 decreased cytoplasmic GR levels and promoted ligand-dependent GR nuclear translocation, thereby altering the GR-mediated stress response [27]. It was reported that Ahi1 expression was reduced in 3xTg AD mice and Alzheimer's disease (AD) model cells, whereas Ahi1 overexpression rescued amyloid pathology in AD model cells [28], and furthermore, AHI1 expression was significantly reduced in serum of AD patients [29]. These studies suggest that Ahi1 may be involved in the pathogenesis of AD, which is clinically characterized by cognitive impairment. However, the mechanism by which prenatal stress leads to cognitive impairment in offspring remains to be further elucidated.

Ahi1 and Huntingtin-associated protein 1 (Hap1) are able to form a stable complex that is critical in early brain development, and the absence of either reduces the expression of the other [30]. Hap1 can interact with WD40 repeat sequence 68 (WDR68)/Dcaf7, a highly conserved protein that is involved in multiple cellular processes, and it binds to dual-specificity tyrosine phosphorylation regulated kinase 1A (DYRK1A) [31]. The *Dyrk1A* gene is located on human chromosome 21, and Dyrk1A protein level is increased in human AD and Down syndrome (DS) brains [32–34]. Transgenic animals overexpressing Dyrk1A exhibit significant cognitive deficits in hippocampus-dependent memory accompanied by neurogenesis deficits and reduced synaptic plasticity, whereas inhibition of DYRK1A attenuates cognitive dysfunction in animal models of DS and AD [35–37]. Therefore, we hypothesized that GR/Ahi1 may regulate WDR68-DYRK1A binding and mediate cognitive impairment in PNS offspring.

In this study, we found that Ahi1 regulates the level of WDR68, and more importantly, Ahi1 and DYRK1A compete for the binding of WDR68. Ahi1 knockout promotes binding of WDR68 and DYRK1A, increases DYRK1A protein level, and Ahi1$^{-/-}$ mice exhibit cognitive impairment and reduced synaptic plasticity. Prenatal stress leads to elevated GC levels and increased GR nuclear translocation in offspring, resulting in decreased Ahi1 levels, increased binding of WDR68 and DYRK1A, and DYRK1A protein levels, with offspring exhibiting reduced synaptic plasticity and cognitive impairment. In addition, RU486 (a GR antagonist), increased Ahi1/GR levels and improved memory impairment and synaptic plasticity in PNS offspring.

Materials and methods

Animals

Ahi1$^{-/-}$ mice were produced according to previously described [26, 38]. Ahi1 floxed mice on a 129vEV/C57BL/6N background (Ahi1$^{loxp/loxp}$) were crossed with mice carrying the EIIa promoter-driven Cre transgene [(The Jackson Laboratory, B6.FVB-Tg (EIIa-Cre) C5379Lmgd/J)], EIIa adenoviral promoter drives expression of Cre recombinase in early mouse embryos, and Cre-mediated recombination occurs in a variety of tissues. The resulting heterozygous mice were used to generate homozygous conditional KO (EIIa-Cre-Ahi1$^{-/-}$) mice in which Ahi1 is deleted in a wide range of tissues including germ cells. Male homozygous KO (EIIa-Ahi1$^{-/-}$) mice were crossed with female wild-type (WT) mice (C57BL/6J) to produce heterozygous (Ahi1$^{+/-}$) mice without EIIa-Cre. Ahi1 heterozygous (Ahi1$^{+/-}$) male and female mice were mated for the production of Ahi1 KO (Ahi1$^{-/-}$) mice and Ahi1 WT mice (Ahi1$^{+/+}$), on the mixed 129vEV/C57BL/6N background. Since our previous study found that there sex differences among Ahi1$^{-/-}$ mice in depression and female Ahi1$^{-/-}$ mice exhibit estrogenic protection [24], for this study, we chose male Ahi1$^{-/-}$ mice for the study. 3-month-old ICR male and female mice were mated and mating pins were used to determine the first gestation day of pregnancy. Pregnant female mice were randomly assigned to either the prenatal stress (PNS) group or the control group (CON). The PNS group was placed individually in well-ventilated 50 mL test tubes without movement to receive restraint pressure from 9:00 to

11:00 am on GD5-GD20, whereas the CON group was left undisturbed. All mice were housed in cages at the Soochow University Experimental Animal Center with a maximum of 5 mice at a temperature of 22 ± 2 °C, 12 h light (7 am to 7 pm)/dark cycle (7 pm to 7 am), and free access to food and water. In addition, we examined the behavior of prenatally stressed 2–3-month-old male and female offspring, and the results showed that the male offspring showed cognitive impairment (Fig. 5), whereas the female offspring did not (Supplementary Fig. 4I-P). Therefore, prenatally stressed male offspring mice were used in this study to investigate the molecular mechanisms. All procedures and protocols for this study were conducted in accordance with the Regulations for the Management of Laboratory Animals and approved through the Institutional Animal Care and Use Committee of Soochow University.

Animal drug administration

Mifepristone (RU486; Sigma-Aldrich Corp., St Louis, MO, USA) was dissolved in normal saline 10% Tween 80 and 10% DMSO, and freshly prepared before treatment. PNS and CON mice were injected intraperitoneally (i.p.) of RU486 (20 mg/kg) or vehicle for 3 weeks. This dose was selected based on previous reports [39, 40].

Morris water maze (MWM) test

The Morris water maze test was conducted as described previously [41, 42]. The Morris water maze was a circular pool (120 cm in diameter and 50 cm high) filled with black opaque water (22 ± 1 °C). The pool was divided into four equal imaginary quadrants with a platform (10 cm in diameter) submerged underwater for 1 cm. Mice were trained once a day in each of the different quadrants for 5 consecutive days. When the mice were placed in the pool, they were allowed to find the platform within 60 s. If the mice did not find the platform within 60 s, they were guided to the platform and allowed to stay on it for 10 s. The escape latency, movement speed and movement distance were recorded by the ANY-maze Video Tracking System (Stoelting Co., USA). On the sixth day of this test, the platform was removed from the pool; the number of times crossing the platform area, and the time spent in the target quadrant were recorded to assess spatial memory.

Novel object recognition (NOR) test

The new object recognition test was performed as previously described [41, 43, 44]. The test was performed in a ($40 \times 40 \times 40$ cm^3) box, and mice were placed in the box for 3 consecutive days for 10 min of adaptation. On the fourth day, two identical objects (object 1 and object2) were placed in the box 5 cm from the side wall and the mice were allowed to explore for 10 min. After 90 min, a familiar object was replaced by a novel object of a different color and shape, and the mice were placed back in the device to freely explore the object for 10 min. Before each trial, the device was washed with a 75% ethanol solution. The behavior of the mice was recorded by the ANY-maze Video Tracking System (Stoelting Co., USA). The preference index is defined as the percentage of time spent on one of the two identical objects versus the time spent on both objects. The recognition index is defined as the percentage of time spent on the new object versus the time spent on exploration familiar and novel objects.

Y maze test

The spontaneous alternating behavior in the Y-maze test is based on a behavioral test of the animal's innate natural exploratory curiosity and is considered to reflect short-term spatial working memory [45, 46]. The Y-maze apparatus was composed of three equal-length arms (30 cm $\times 5$ cm $\times 15$ cm) made of opaque plastic with an angle of 120° from each other (labeled A, B and C). The mice were placed in the center of the Y-maze and allowed to freely explore the arms for 8 min and monitored by the ANY-maze Video Tracking System (Stoelting Co., USA). Arm entry was defined as all four arms entering the Y maze in one arm. Spontaneous alternations were recorded manually when mice entered all three different arms (i.e., ABC, ACB, CAB, BCA, CBA, and BAC). The percentage of spontaneous alternations (%) was defined as the number of spontaneous alternations in the behavior/(total number of arms entered $-2) \times 100\%$. After each trial, the Y maze needs to be cleaned with 75% ethanol solution to eliminate any odor that might have been left by the previous subjects.

Open field test

The open field test was performed as described previously [47]. The open field apparatus contained a plastic box ($40 \times 40 \times 40$ cm^3) with a central area of (20×20 cm^2). Mice were placed in the center of the apparatus and center entries, their total time spent in the inside area and distance of movement were recorded by the ANY-maze Video Tracking System (Stoelting Co., USA) for 6 min. After each test, the device needs to be cleaned with 75% ethanol solution.

Elevated plus maze test

The elevated positive maze (EPM) consisted of two opposing closed and open arms (30×5 cm^2), with the closed arm being 14 cm high [47]. To begin a trial, the mice were gently placed in the center of the maze facing the open arms and the

time spent on the open and closed arms and the distance of movement on the open arms were recorded by ANY maze video tracking system (Stoelting Co., USA) for 10 min. After each trial, the maze needed to be cleaned with a 75% ethanol solution.

Light–dark box test

The light–dark box experiment is based on the conflict between the animal's innate aversion to illuminated areas and spontaneous exploratory activity [48, 49]. The apparatus consisted of a polypropylene cage with dimensions of $45 \times 27 \times 30$ cm^3 with two compartments, which were separated by a divider with a 7×7 cm^2 opening at the floor level. The larger compartment (27×27 cm^2) was open-topped, transparent and brightly illuminated (900 lx), while the smaller compartment (18×27 cm^2) had black walls covered with black Plexiglass on top. For each test, mice were placed in the center of the dark compartment and the time spent in the light compartment and the number of transitions between the two compartments were recorded by ANY maze video tracking system (Stoelting Co., USA) for 5 min. The apparatus was thoroughly cleaned with 75% alcohol after each trial.

Rotarod test

Motor coordination of mice was assessed by Rotarod apparatus (Zhenghua, Anhui Province, China). The Rotarod test was performed as previously described [47]. Mice were trained three times for 5 min at 5 rpm on two consecutive days, and on the third day, the rotating rod was set to accelerate from 0 to 40 rpm in 5 min. Each mouse was tested three times with a 5-min rest period for each trial. The latency to fall from the rotating rod was the average of the three trials.

Recording of long-term potentiation (LTP)

Mice were anesthetized with isoflurane and rapidly decapitated and placed in pre-cooled oxygenated (95% O$_2$, 5% CO$_2$) dissection buffer containing 5 mM KCl, 1.25 mM NaH$_2$PO$_4$, 26 mM NaHCO$_3$, 212.7 mM Sucrose, 10 mM glucose, 1 mM CaCl$_2$, and 3 mM MgCl$_2$ (pH 7.4). Coronal hippocampal slices (400 μm) were prepared from the resected brains of mice using a vibratome (Leica VT1200S). Slices were bubbled with oxygenated artificial cerebrospinal fluid (ACSF) consisting of 5 mM KCl, 124 mM NaCl, 26 mM NaHCO$_3$, 2.4 mM CaCl$_2$, 1.25 mM NaH$_2$PO$_4$, 1.2 mM MgCl$_2$ and 10 mM glucose (pH 7.4) for 30 min at both 32 °C and room temperature, and then transferred to a submersion recording chamber, which was continuously perfused oxygenated ACSF at a rate of 1 mL/min. Field excitatory postsynaptic potentials (fEPSP) were recorded from CA1

neurons by stimulating CA3 neurons. LTP was induced by applying high frequency stimulation (HFS) (four 100 Hz and 1 s trains delivered 20 s apart). LTP amplitude was quantified as the percentage change in fEPSP slope (40%) during the 60-min interval after LTP induction. The electrophysiological data were acquired with an Axon multiclamp 700B amplifier, filtered at 10×10^4 kHz, and digitized at 10 kHz, and the slope and peak amplitude of fEPSP were measured and analyzed offline using pClamp 10.3 software (Molecular Devices Corp, USA). Paired-pulse facilitation (PPF) is a short-term synaptic plasticity assessed at inters-stimulus intervals (ISIs) of 25, 50, 75, 100, 125, 150 and 200 ms. The paired pulse ratio was determined as the ratio between the second pulse and the first pulse of the fEPSP.

Serum corticosterone measurement

Measurement of serum corticosterone was performed according to the previous study [50]. Briefly, blood was collected through the corneal vessels of mice from 9 to 10 am and kept at room temperature for 1 h, then centrifuged at 3000 rpm for 10 min. The serum (supernatant fraction) was transferred to a new tube for subsequent assays. Serum corticosterone level was measured with commercially available ELISA kit (ml037564; mlbio, China) according to the manufacturer's instructions.

Primary hippocampal neuron culture

The day before primary hippocampal neurons were isolated, plates were coated with 0.1 mg/mL poly-D-lysine at 37 °C overnight. The next day, the poly-D-lysine was removed and washed three times with PBS. Female mice at 16.5 days of gestation were anesthetized and executed by cervical dislocation. Hippocampal tissue from fetal mice was isolated and the meninges were removed under a microscope. The hippocampal tissue was digested with 0.125% trypsin at 37 °C for 15 min, and then the reaction was terminated with DMEM supplemented with 10% FBS. The suspension was filtered through a 70 μm filter and centrifuged at 1000 rpm for 5 min. Cell precipitates were resuspended in the neurobasal medium supplemented with 2% B27 and 0.5 mmol/L L-glutamine, and neurons were replaced with half of fresh medium every 3 days.

Western blot analysis

Fresh mouse hippocampal tissue and PC12 cells were collected and lysed in RIPA lysis buffer (P0013B, Beyotime, Shanghai, China). The solution was centrifuged at 16,000×g for 30 min at 4 °C. The supernatant solution was gently collected and the protein concentration was determined by the BCA kit. 20–40 μg protein samples were electrophoresed

and electro-transferred to nitrocellulose membranes (Millipore, Germany) as we described previously [51]. The membranes were blocked with 5% milk in phosphate-buffered saline/0.1% Tween 20 (PBST) for 1 h to remove non-specific binding and incubated with primary antibodies overnight at 4 °C with shaking. After washing the membrane with PBST, the membrane blots were detected using an ECL chemiluminescence system (Tanon-5200, Shanghai, China) and the density of the bands was analyzed by Alpha Ease image analysis software (version 3.1.2). Primary antibodies were Ahi1 (sc-515382,1:500), Ubiquitin (sc-166553,1:600), His-probe antibody (sc-53073,1:1000) (Santa Cruz Biotechnology, Delaware, CA, USA); GR (A5387,1:1000), β-actin (A5538, 1:5000), β-tubulin (A5167, 1:5000) (Bimake, Houston, TX, United States); DYRK1A (8765,1:1000) (Cell Signaling Technology Inc., Danvers, MA, USA); WDR68 (ab138490) and Histone3 (ab1791) (Abcam, Cambridge, MA, USA); Myc Tag (Abmart, M20002H, 1:3000); PSD95 (20665-1-AP, 1:1000), Synaptophysin (17785-1-AP, 1:1000) (Proteintech, Wuhan, China).

Immunofluorescence staining

Immunofluorescence staining was performed as described previously [27]. Mice were perfused through the heart with ice-cold saline and 4% paraformaldehyde through the heart. The brains of mice were collected, post-fixed for 24 h and dehydrated in a solution of 15% and 30% sucrose (w/v), and brain tissue was cut into coronal slices (12 μm) using a cryostat. Brain slices were washed with phosphate buffered saline (PBS) and treated with 0.3% Triton X-100/3% bovine serum albumin/PBS for 1 h at room temperature. Brain slices were incubated with the primary antibody overnight at 4 °C. The next day, sections were incubated with the secondary antibody and the nuclear dye DAPI for 1 h at 4 °C. All images were captured using a fluorescence microscope (Axio ScopeA1, Carl Zeiss, Oberkochen, Germany).

Quantitative polymerase chain reaction (Q-PCR)

Fresh hippocampal tissue from mice was collected and total RNA was extracted from the mouse brain using the RNeasy Plus Mini kit according to the instructions. The cDNA was synthesized by reverse transcription using the Transcription Factor First Strand cDNA Synthesis Kit as described previously [24]. Real-time PCR was performed by a 7500 real-time PCR machine (Applied Biosystems, USA) in a 20 μL volume containing 50 ng cDNA, 10 μL 2XSYBR Green PCR Master Mix and 1 μL primers (10 μM) and water. GAPDH was used as an internal control. The primer sequences are listed in Supplementary Table 1.

Co-immunoprecipitation (Co-IP)

Fresh hippocampal tissue was homogenized in lysis buffer and the homogenate centrifuged at 16,000×g for 30 min at 4 °C, The supernatant was collected and the concentration was determined by the BCA method. The 500 μg protein sample was pre-absorbed with 50 μL Protein G agarose beads (16–266, Millipore) for 2 h at 4 °C. After centrifugation at 1000×g for 2 min, the supernatant was incubated with 5 μg Ahi1 antibody, WDR68 antibody, DYRK1A antibody or IgG (as a negative control) at 4 °C overnight. The next day, 50 μL protein G agarose beads were added to the homogenate and incubated at room temperature for 2 h. Beads were collected by centrifugation at 1000×g for 2 min. After washing with lysis buffer, the beads were eluted with sample buffer containing SDS and the samples were heated at 96 °C for 10 min for further Western blot analysis.

Golgi staining for dendritic spines

To assess changes in neuronal dendritic spines, we performed Golgi-Cox staining by using the FD Fast Golgi Staining Kit (FD Neuro Technologies, Columbia, MD, USA) performed according to the manufacturer's instructions. Images of CA1 and DG hippocampal pyramidal neurons were observed using a Pannoramic MIDI scanner (3DHistech Ltd., Budapest, Hungary) equipped with a GS3-U3-51S5M-C camera (FLIR, Canada). The morphology of the selected neurons was reconstructed and analyzed using ImageJ (National Institutes of Health, Bethesda, USA) and NeuronStudio (Version 0.9.92) software as described previously [52], and the second or third dendritic branch of apical spines of hippocampal DG and CA1 neurons were selected for Sholl analysis. Images of stained spines were obtained from a NIKON Eclipse ci microscope with NIS Elements Viewer software. In this study, data from 3 brain slices per animal with 5 neurons per slice were averaged and used for further statistical analysis. We calculated the spine density expressed as the number of spines per 10 μm branch, and the number of dendrites was counted by a double-blind method.

Plasmid or siRNA transfection

Ahi1 or DYRK1A cDNAs were inserted into the pCDNA3.1-His vector, Hap1 cDNA was inserted into the pCDNA3.1-Myc vector. siRNAs against Ahi1 were synthesized by Gene Pharma with the following sequences, respectively: 5′-GCCACCUCAAUAUCAUUUATT-3′ and 5′-UAAAUGAUAUUGAGGUGGCTT-3′. The Plasmids or siRNA brought into the PC12 or Hela cells by transient transfection

with lipofectamine 2000 (Invitrogen, Carlsbad, CA, USA) according to the manufacturer's instructions.

Nuclear and cytoplasmic extraction

Mice were executed by cervical dislocation and hippocampal tissue was collected by dissection on ice. The tissue was homogenized using a glass homogenizer to disrupt cell membranes and release cytoplasm. Nuclear Protein Extraction Kit (P0028, Beyotime Biotechnology, Shanghai, China) was used for nuclear and cytoplasmic extraction. Cell fractions were extracted according to the manufacturer's kit manual.

Statistical analysis

All data are presented as mean $\pm$ SEM. GraphPad Prism 8.0 (GraphPad Software, Inc.) was used for data analysis. Differences between the two groups were determined by Student's t-test. The differences between the two groups conformed to a normal distribution before Student's t-test. Differences between groups were compared with two-way analysis of variance followed by Bonferroni's multiple comparisons post hoc test or one-way analysis of variance followed by Tukey's multiple comparison tests. All differences were considered statistically significant when $P < 0.05$. P values are indicated with an asterisk as follows: *$P < 0.05$; **$P < 0.01$; ***$P < 0.001$ and ****$P < 0.0001$.

Results

Ahi1$^{-/-}$ mice exhibit cognitive impairment and reduced synaptic plasticity

To further explore the relationship between Ahi1 and cognitive impairment and the possible mechanisms, we tested whether Ahi1$^{-/-}$ mice have cognitive impairment by behavioral experiments. In this study, we found that the level of Ahi1 did not differ between Ahi1 WT mice (Ahi1$^{+/+}$) and Ahi1 heterozygous mice (Ahi1$^{+/-}$), and we chose Ahi1$^{+/+}$ mice as a control to study the phenotype of Ahi1$^{-/-}$ mice (Supplementary Fig. 1A-B). In the MWM test, Ahi1$^{-/-}$ mice exhibited impairment of learning in locating the invisible
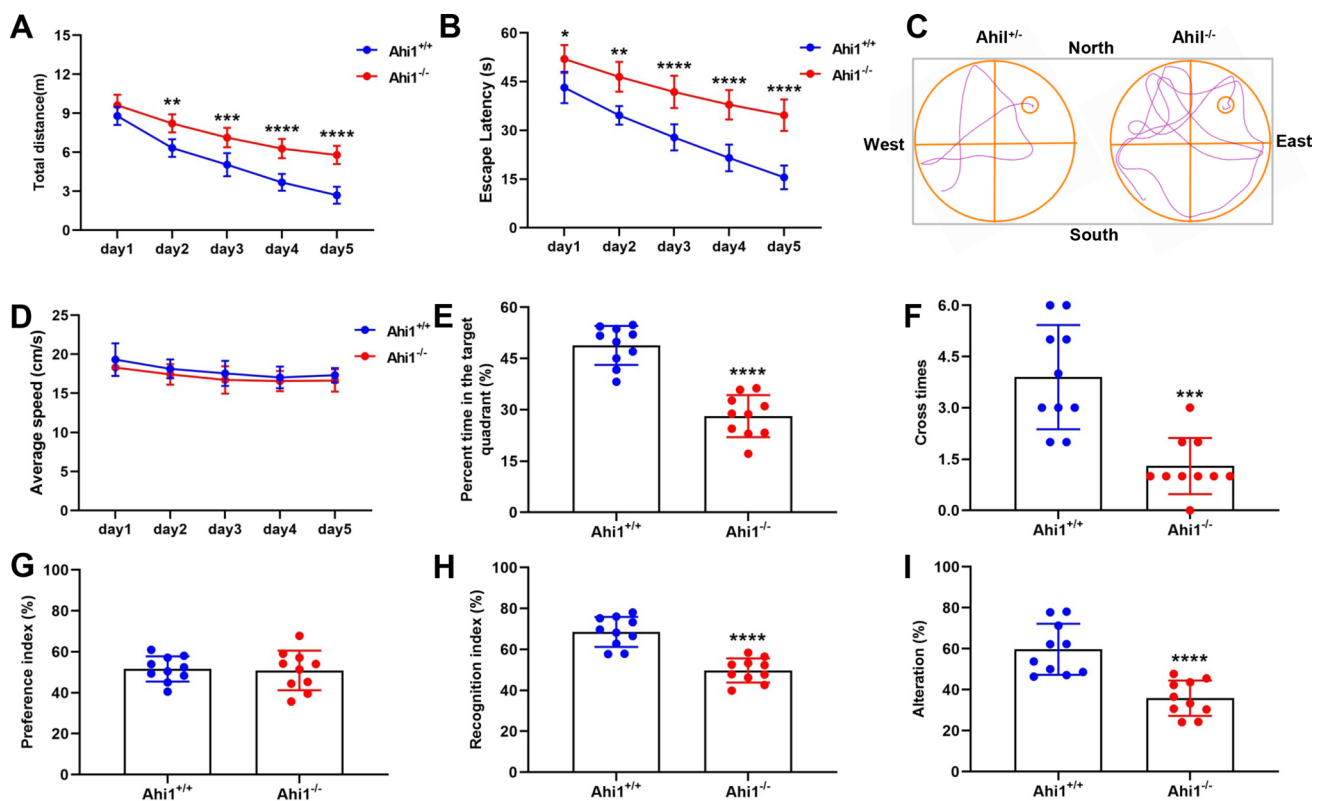

Fig. 1 Ahi1$^{-/-}$ mice exhibit cognitive impairment. Behavioral tests were performed in 2–3 month-old mice. In the MWM test, movement distance (**A**), escape latency (**B**) representative images of swimming paths (**C**), movement speed (**D**), time spent in the target quadrant (**E**) and number of times crossing the platform area (**F**) were recorded. N=10 mice. In the NOR test, preference index (**G**) and recognition index (**H**) were recorded. N=10 mice. In the Y-maze test, the percentage of spontaneous alternations was recorded. N=10 mice (**I**). *$P < 0.05$; **$P < 0.01$; ***$P < 0.001$; ****$P < 0.0001$

platform as indicated by increased movement distance and escape latency compared to Ahi1$^{+/+}$ mice (Fig. 1A–C), whereas they movement speed was not significantly different (Fig. 1D). In the probe trial, Ahi1$^{-/-}$ mice showed impairment in spatial memory retention as indicated by that Ahi1$^{-/-}$ mice spent less time in the target quadrant and fewer number of times crossing the platform area (Fig. 1E, F). In NOR test, there were no significant differences in preference index between Ahi1$^{-/-}$ and Ahi1$^{+/+}$ mice during the training phase, indicating that these objects do not affect the exploratory behavior of mice (Fig. 1G). In the testing phase, Ahi1$^{-/-}$ mice show a decreased recognition index than Ahi1$^{+/+}$ mice (Fig. 1H), indicating cognitive impairment in Ahi1$^{-/-}$ mice. In the Y-maze test of short-term spatial memory, the percentage of spontaneous alternations was significantly reduced in Ahi1$^{-/-}$ mice compared to Ahi1$^{+/+}$

mice (Fig. 1I). In conclusion, Ahi1$^{-/-}$ mice exhibited significant cognitive impairment.

Accumulating evidence suggests that synaptic plasticity is associated with cognitive function [53–55]. Thus, we investigated whether Ahi1 knockout affects hippocampal synaptic plasticity. Synaptic plasticity is measured by changes in synaptic strength, and LTP, the sustained enhancement of synaptic strength, is strongly associated with learning and memory [45, 56]. In our study, Ahi1$^{-/-}$ mice showed lower LTP compared to Ahi1$^{+/+}$ mice (Fig. 2A–C) indicated by a significant reduction in fEPSP slope (Fig. 2B) and fEPSP peak amplitude (Fig. 2C). Meanwhile, PPF was immediately measured, and there was no significant difference between the two groups (Fig. 2D). These results suggest that Ahi1 knockout reduces LTP. Loss of hippocampal dendritic spines leads

Fig. 2 Ahi1$^{-/-}$ mice exhibit reduced synaptic plasticity. LTP was recorded using acute hippocampal slices from Ahi1$^{-/-}$ and Ahi1$^{+/+}$ mice. The effects of HFS on the fEPSP initial slope (**A**), cumulative data for the mean slope of fEPSP 60 min post-HFS (**B**), cumulative data for the mean peak amplitude of fEPSP 60 min post-HFS (**C**) and the PPF ratio of each group (**D**) were recorded. N = 6 mice. Representative micrographs of DG and CA1 dendritic spines in the hippocampus of Ahi1$^{-/-}$ and Ahi1$^{+/+}$ mice (**E**). Spine densities of DG and CA1 in the hippocampus of Ahi1$^{-/-}$ and Ahi1$^{+/+}$ mice were analyzed. N = 4 mice (**F**, **G**). Western blot analysis revealed that synaptophysin and PSD95 were reduced in the hippocampus of Ahi1$^{-/-}$ mice compared to Ahi1$^{+/+}$ mice. N = 6 mice. Scale bar = 10 μm. ***$P < 0.001$; ****$P < 0.0001$
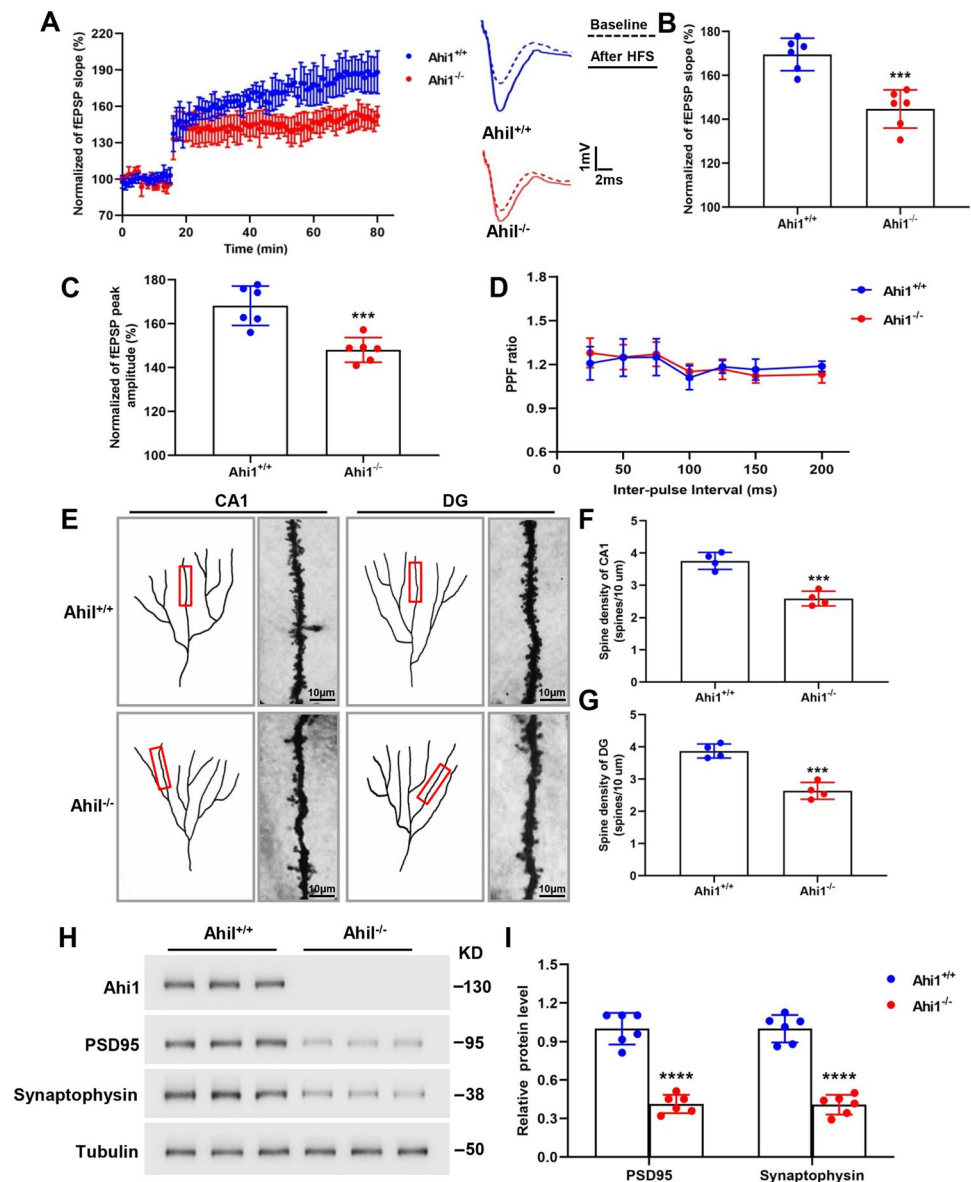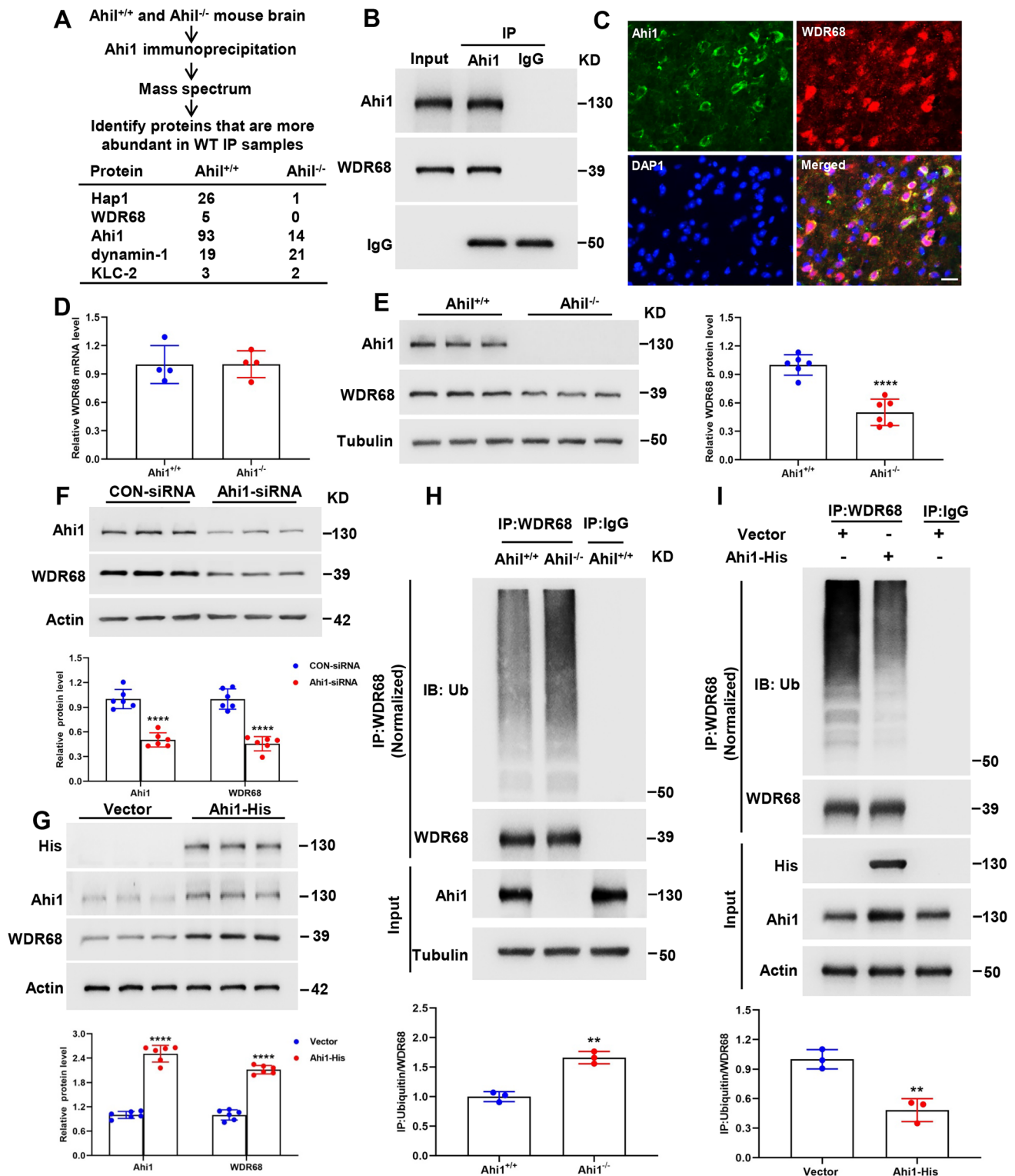
to LTP and cognitive impairment [45, 57]. We therefore investigated whether Ahi1 knockout affects hippocampal dendritic spines by Golgi staining. Spine density in CA1 and DG of Ahi1$^{-/-}$ mice was significantly reduced compared to Ahi1$^{+/+}$ mice (Fig. 2E–G). The results suggest that Ahi1 knockout resulted in spine loss in the hippocampal region. In addition, the levels of synaptophysin (a specific marker for presynaptic terminals) and PSD95 (a membrane-associated proteins in the postsynaptic density) in the hippocampus of Ahi1$^{-/-}$ mice was

◄**Fig. 3** Ahi1 stabilizes WDR68 protein levels by inhibiting its degradation. Ahi1$^{-/-}$ and Ahi1$^{+/+}$ mice brain tissue lysates were precipitated with anti-Ahi1 and analyzed for potential Ahi1-binding proteins by mass spectrometry (**A**). In vivo binding of WDR68 to Ahi1 was verified by Western blotting with anti-Ahi1 in immunoprecipitates from Ahi1$^{+/+}$ mouse brain tissue (**B**). Coimmunostaining of Ahi1 and WDR68 in the brain of Ahi1$^{+/+}$ mouse (**C**). Scale bar = 10 µm. Q-PCR showed no difference in WDR68 mRNA levels in the hippocampus of Ahi1$^{-/-}$ and Ahi1$^{+/+}$ mice. N = 4 mice (**D**). Western blotting showed a significant reduction in WDR68 protein levels in the hippocampus of Ahi1$^{-/-}$ mice. N = 6 mice (**E**). After Ahi1-siRNA transfection of PC12 cells for 48 h, the level of WDR68 protein drastically decreased. N = 6 cell samples (**F**). PC12 cells were transfected with Ahi1-His plasmid or vector for 48 h, and overexpression of Ahi1 significantly increased the level of WDR68 protein. N = 6 cell samples (**G**). Hippocampal tissues from Ahi1$^{-/-}$ and Ahi1$^{+/+}$ mice were collected and immunoprecipitated with WDR68 antibody, and Western blotting demonstrated a significant increase in ubiquitinated WDR68 protein. N = 3 mice (**H**). PC12 cells transfected with Ahi1-His plasmid or vector were collected and immunoprecipitated with WDR68 antibody, and Western blotting showed that ubiquitinated WDR68 protein was significantly reduced. N = 3 cell samples (**I**). **$P < 0.01$; ****$P < 0.0001$

decreased in comparison to Ahi1$^{+/+}$ mice (Fig. 2H, I). All these results suggest that Ahi1$^{-/-}$ mice exhibit reduced synaptic plasticity.

Ahi1 stabilizes WDR68 protein levels by inhibiting its degradation

To investigate the mechanism by which Ahi1 deficiency leads to cognitive impairment, we performed Ahi1 immunoprecipitation of brain tissues from Ahi1$^{+/+}$ and Ahi1$^{-/-}$ mice to reveal Ahi1-interacting proteins, which should be more abundant in Ahi1$^{+/+}$ samples than in Ahi1$^{-/-}$ samples. As expected, we saw more Hap1 and Ahi1 in Ahi1$^{+/+}$ immunoprecipitates than in Ahi1$^{-/-}$ immunoprecipitates. In addition, WDR68, also known as Dcaf7, a highly conserved scaffolding protein containing five WD40 repeats important for craniofacial development [58, 59], was only present in Ahi1$^{+/+}$ immunoprecipitates and was not detected in Ahi1$^{-/-}$ immunoprecipitates (Fig. 3A). We further confirmed the interaction between WDR68 and Ahi1 by coimmunoprecipitation and coimmunostaining (Fig. 3B, C). Next, we examined whether Ahi1 regulates WDR68 levels. The mRNA level of WDR68 in the hippocampus of Ahi1$^{-/-}$ mice was not altered compared to Ahi1$^{+/+}$ mice (Fig. 3D), while the protein of WDR68 in the hippocampus of Ahi1$^{-/-}$ mice was significantly decreased compared to Ahi1$^{+/+}$ mice (Fig. 3E). This suggests that Ahi1 stabilizes WDR68 at the protein level. Knockdown of Ahi1 in PC12 cells also induced a significant decrease in WDR68 protein levels, while overexpression of Ahi1 in PC12 cells induced an increase in WDR68 protein levels (Fig. 3F, G). We then evaluated the WDR68 half-life after knockdown or overexpression of Ahi1 in PC12 cells. The half-life of endogenous WDR68 was significantly shortened by knockdown of Ahi1 (Supplementary

Fig. 2A). Consistent with this, overexpression of Ahi1 significantly prolonged the half-life of endogenous WDR68 compared to the control vector (Supplementary Fig. 2B). Previous studies have shown that WDR68 is degraded mainly through the ubiquitin–proteasome system (UPS) [31]. To further whether Ahi1 inhibits the degradation of WDR68, we compared the degradation of WDR68 in the hippocampus of Ahi1$^{-/-}$ mice and Ahi1$^{+/+}$ mice. The results demonstrated that ubiquitination degradation of WDR68 was remarkably increased in the hippocampal tissues of Ahi1$^{-/-}$ mice compared to Ahi1$^{+/+}$ mice (Fig. 3H). In addition, we overexpressed Ahi1 in PC12 cells and found that polyubiquitinated WDR68 was significantly reduced (Fig. 3I). Thus, we conclude that Ahi1 not only binds WDR68 but also stabilizes its levels by inhibiting its degradation.

DYRK1A and Ahi1 compete for WDR68 binding and its protein level is elevated in hippocampal tissue of Ahi1$^{-/-}$ mice

In this study, we found that the mRNA level of DYRK1A in the hippocampus of Ahi1$^{-/-}$ mice was unchanged compared with Ahi1$^{+/+}$ mice (Fig. 4A), whereas the protein level of DYRK1A in the hippocampus of Ahi1$^{-/-}$ mice was significantly increased compared to Ahi1$^{+/+}$ mice (Fig. 4B). Similarly, knockdown of Ahi1 in PC12 cells resulted in up-regulation of DYRK1A protein levels (Fig. 4C), whereas overexpression of Ahi1 in PC12 cells resulted in down-regulation of DYRK1A protein levels (Fig. 4D). Next, we further investigated whether Ahi1 and DYRK1A could competitively or synergistically interact with WDR68. The results showed increased binding between WDR68 and DYRK1A in the hippocampal tissues of Ahi1$^{-/-}$ mice compared to Ahi1$^{+/+}$ mice (Fig. 4E). These results suggest that there may be competition for WDR68 binding between Ahi1 and DYRK1A and that WDR68 binding may be important for DYRK1A stability. Ahi1 deficiency promotes WDR68 binding to DYRK1A and up-regulates DYRK1A levels. To further confirm that Ahi1 and DYRK1A compete for WDR68 protein binding, we overexpressed Ahi1 or DYRK1A in PC12 cells to observe the effect on WDR68 binding. As expected, overexpression of Ahi1 inhibited the binding of DYRK1A and WDR68 (Fig. 4F), while overexpression of DYRK1A inhibited the binding of Ahi1 and WDR68 (Fig. 4G). Thus, our results suggest that Ahi1 and DYRK1A compete for WDR68 protein binding and regulate DYRK1A levels.

Prenatal stress leads to cognitive impairment in male offspring

It is now widely recognized that the developing fetus is susceptible to perturbations in the intrauterine environment
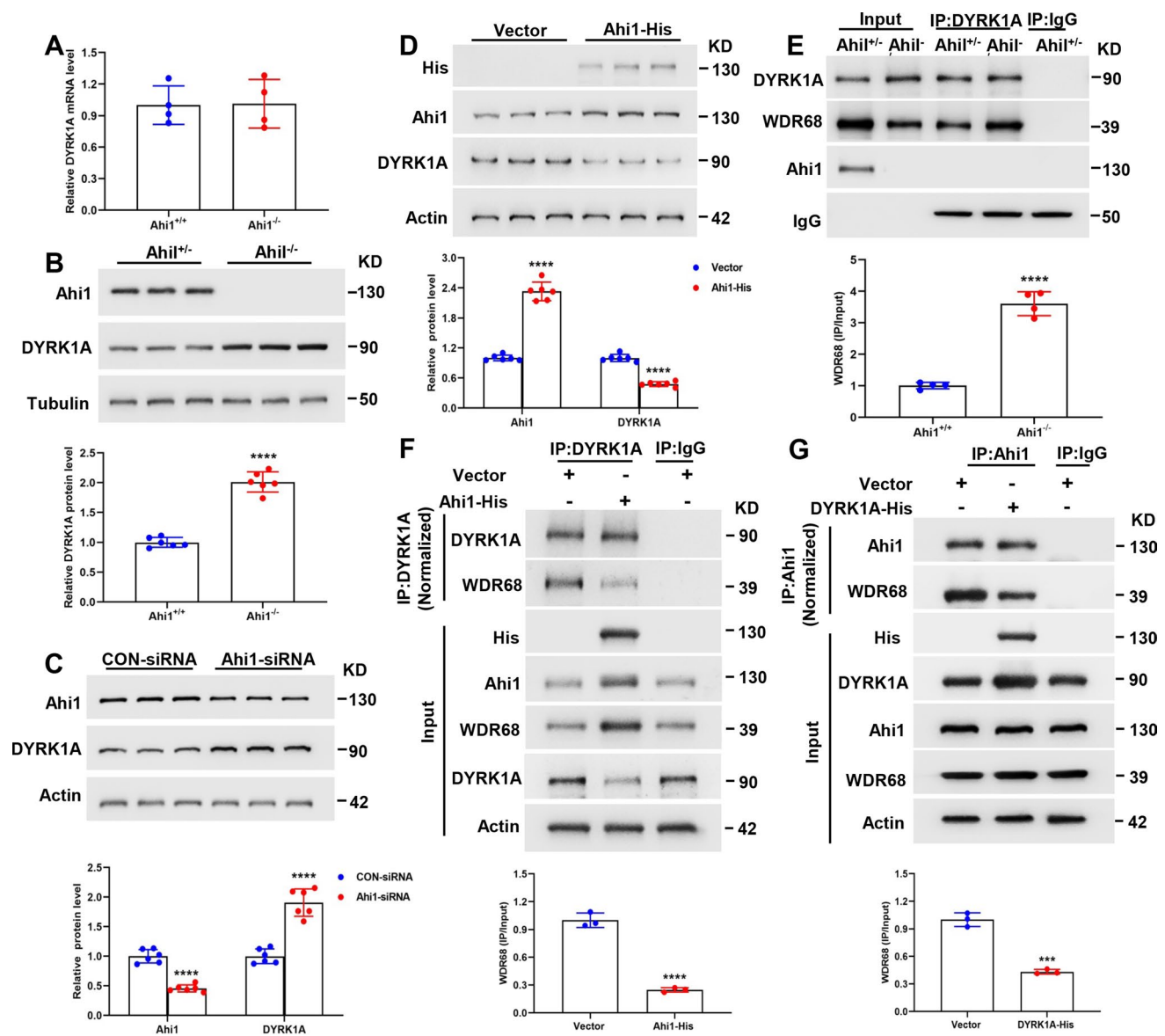
Fig. 4 DYRK1A and Ahi1 compete for WDR68 binding and its protein level is elevated in hippocampal tissue of Ahi1$^{-/-}$ mice. Q-PCR showed no difference in DYRK1A mRNA levels in the hippocampus of Ahi1$^{-/-}$ and Ahi1$^{+/+}$ mice. N=4 mice (**A**). Western blotting showed that DYRK1A protein was significantly elevated in the hippocampus of Ahi1$^{-/-}$ mice. N=6 mice (**B**). Transfection of Ahi1-siRNA into PC12 cells for 48 h significantly up-regulated DYRK1A protein levels. n=6 cell samples (**C**). Transfection of Ahi1-His plasmid into PC12 cells for 48 h significantly down-regulated the level of DYRK1A protein. n=6 cell samples (**D**). Hippocampal tissues from Ahi1$^{-/-}$ and Ahi1$^{+/+}$ mice were collected and immunoprecipitated with DYRK1A antibody, and Western blotting revealed increased binding between DYRK1A and WDR68. N=4 mice (**E**). PC12 cells transfected with Ahi1-His plasmid or vector were collected and immunoprecipitated with DYRK1A antibody, and Western blotting showed that overexpression of Ahi1 reduced the binding of DYRK1A and WDR68. N=3 cell samples (**F**). PC12 cells transfected with DYRK1A-His plasmid or vector were collected and immunoprecipitated with Ahi1 antibody, and Western blotting showed that overexpression of DYRK1A drastically reduced the binding of Ahi1 and WDR68. N=3 cell samples (**G**). ***$P < 0.001$; ****$P < 0.0001$

and that prenatal stress increases the risk of adult diseases in offspring, such as high blood pressure, type 2 diabetes, anxiety disorders, depression, and cognitive impairment [3, 60–64]. Prenatal stress induces excess glucocorticoids to pass through the placenta into the fetus, perturbing the HPA axis in the offspring, leading to lower birth weight and

behavioral changes in adulthood [10, 65, 66]. In this study, we found that PNS offspring mice had reduced birth weight compared to controls (Fig. 5A), but prenatal stress did not alter litter size (Fig. 5B). In addition, we found that serum corticosterone levels were significantly higher in PNS offspring compared to controls (Fig. 5C). Next, we investigated
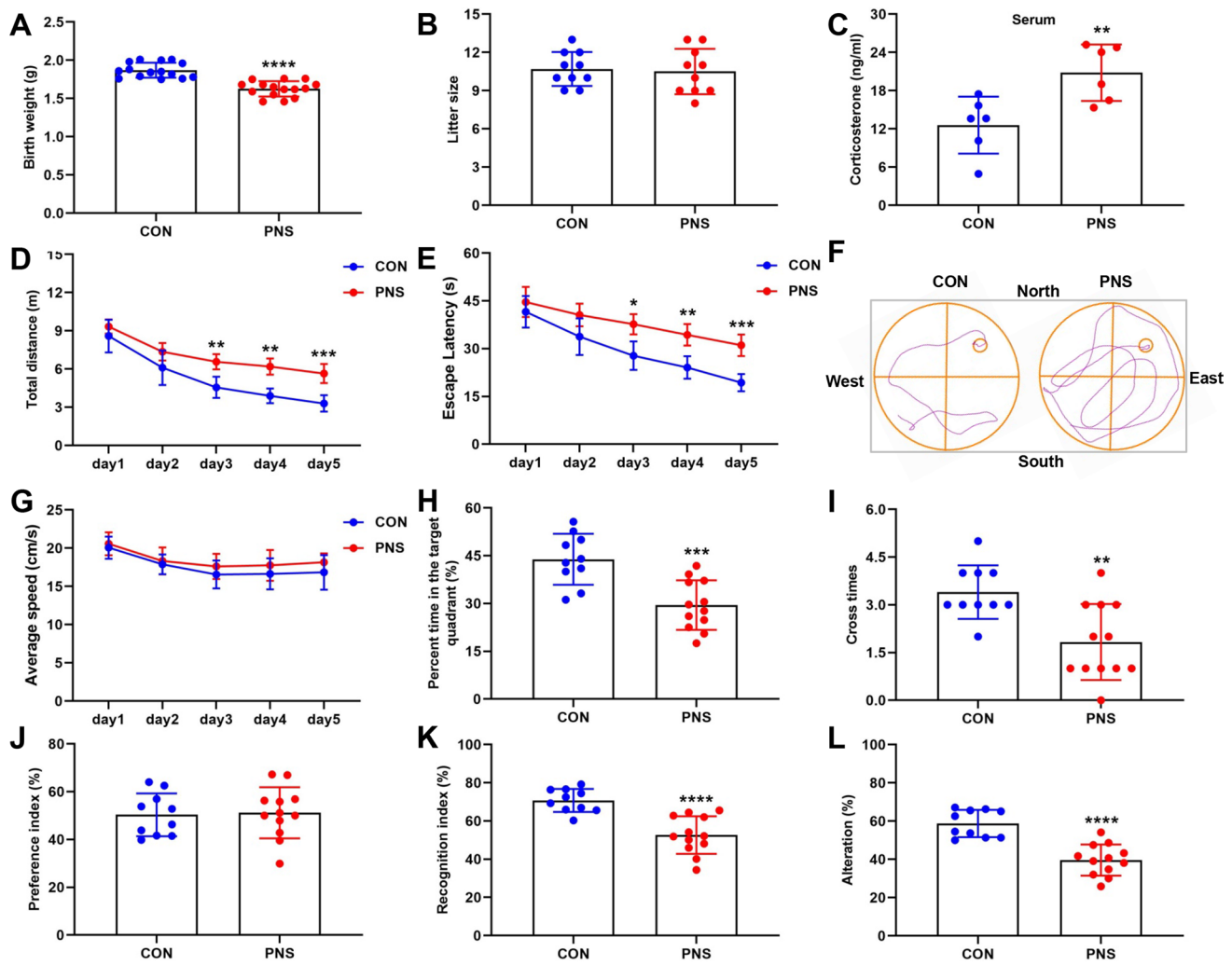
Fig. 5 Prenatal stress leads to cognitive impairment in male offspring. Body weights of CON mice and PNS were recorded at postnatal 1 day. N = 15 mice (**A**). The number of litters in CON mice and PNS was recorded. N = 10 mice (**B**). Serum corticosterone levels were measured by an ELISA method in CON mice and PNS mice. N = 6 mice (**C**). Behavioral tests were performed in 2–3 month-old mice. In the MWM test, movement distance (**D**), escape latency (**E**) represent- ative images of swimming paths (**F**), movement speed (**G**), time spent in the target quadrant (**H**) and number of times crossing the platform area (**I**) were recorded. N = 10–12 mice. In the NOR test, preference index (**J**) and recognition index (**K**) were recorded. N = 10–12 mice. In the Y-maze test, the percentage of spontaneous alternations was recorded. N = 10–12 mice (**L**). *$P < 0.05$; **$P < 0.01$; ***$P < 0.001$; ****$P < 0.0001$

whether adult male offspring mice with PNS had abnormal behavior. In the MWM test, the PNS group showed increased movement distance and escape latency compared to the control group (Fig. 5D–F), indicating that the PNS mice exhibited learning impairment in locating the invisible platform, while there was no significant difference in movement speed between the two groups (Fig. 5G). In the probe trial, the PNS group showed impairment in spatial memory retention as indicated by the PNS group spent less time in the target quadrant and fewer number of times crossing the platform area (Fig. 5H, I). In the NOR test, there was no significant difference in the preference index between PNS and Control groups during the training phase (Fig. 5J), indicating that these objects did not affect the exploratory behavior of the

two groups. In the testing phase, the recognition index of the PNS group was lower than Control group (Fig. 5K), which indicated that the PNS group had cognitive impairment. In the Y-maze test, the percentage of spontaneous alternations was significantly lower in the PNS group of mice compared to the Control group (Fig. 5L). In conclusion, the male offspring of PNS mice showed significant cognitive impairment in adulthood. In addition, we investigated whether prenatal stress-induced male offspring mice exhibit other behaviors. In the open field test, there were no differences between the PNS and control groups in movement distance, center entries and total time spent in the inside area or outside area (Supplementary Fig. 3A-C). In the light–dark box test, there was no difference in light–dark transitions and the time spent

in the light compartment (Supplementary Fig. 3D, E). In the elevated plus maze test, there was no difference in time and distance between the PNS and control groups in the open arm (Supplementary Fig. 3F, G). In the Rotarod test, there was no difference in the latency to fall between the PNS and Control groups (Supplementary Fig. 3H). In addition, we found that there was no difference in body weight between the PNS group and the control group at 2 months of age (Supplementary Fig. 3I). These results suggest that the male offspring of prenatal stress did not exhibit anxiety-like behaviors and motor deficits. In addition, we found no differences in anxiety-like behaviors (Supplementary Fig. 4A-G) motor performance (Supplementary Fig. 4H) and cognition (Supplementary Fig. 4I-P) in prenatally stressed female offspring compared to control female offspring mice.

Prenatal stress alters GR/Ahi1-WDR68-DYRK1A signaling, resulting in decreased binding of Ahi1 to WDR68 and increased binding of WDR68 to DYRK1A

To further investigate the pathogenesis of prenatal stress offspring, we detected GR/Ahi1-WDR68-DYRK1 signaling changes in the hippocampus of PNS offspring. It was found that Ahi1, GR and WDR68 expression were decreased in the hippocampus of the PNS group, while DYRK1A level was elevated compared with the control group (Fig. 6A). Our previous study found that glucocorticoid-like ligand treatment or stress resulting in massive GR nuclear transloca-tion reduced GR binding to cytoplasmic Ahi1 and facilitated nuclear translocation of GR, leading to Ahi1 degradation [27]. In this study, we also found an increase in GR nuclear translocation in hippocampal tissue of the PNS group (Supplementary Fig. 5A, B), which in turn caused a decrease in Ahi1 levels. Next, we further investigated the effects of prenatal stress on Ahi1 and WDR68 binding as well as DYRK1A and WDR68 binding in hippocampal tissues of offspring. Our study found that prenatal stress resulted in decreased Ahi1 and WDR68 binding (Fig. 6B) and increased DYRK1A and WDR68 binding (Fig. 6C) in the hippocam-pus of offspring mice. A growing number of studies have shown that prenatal stress or glucocorticoid exposure is associated with cognitive impairment in offspring [67–69], and our study also found elevated glucocorticoids in PNS offspring. To further investigate the mechanism by which glucocorticoid exposure leads to cognitive impairment, we administered the synthetic glucocorticoid dexamethasone (Dex) to PC12 cells or primary hippocampal neurons for 72 h and found that the expression of Ahi1, GR and WDR68 was decreased, while the expression of DYRK1A was ele-vated in the Dex-treated PC12 cells or primary hippocam-pal neurons compared to the control group (Fig. 6D, Sup-plementary Fig. 6A). In addition, we also found a decrease

in Ahi1 and WDR68 binding and an increase in DYRK1A and WDR68 binding in Dex-treated PC12 cells or primary hippocampal neurons (Fig. 6E, F, Supplementary Fig. 6B-C). These results further confirm that Ahi1 and DYRK1A compete for binding to WDR68.

RU486 increases hippocampal GR and Ahi1 levels and improves synaptic plasticity and cognitive impairment in prenatally stressed offspring

RU486 (mifepristone) is a GR antagonist that blocks deg-radation of Ahi1 in Dex treatment, and increasing evidence suggests that RU486 improves cognition [27, 70, 71]. In this study, we investigated the ameliorative effects of RU486 on cognitive impairment in prenatally stressed offspring. We divided PNS mice and control mice into four groups CON (Control) + VEH (vehicle), CON+RU486, PNS+VEH, PNS+RU486. In the MWM test, the PNS+RU486 group showed decreased movement distance and escape latency compared to the PNS+VEH (Fig. 7A–C), whereas there was no significant difference in movement speed between the four groups (Fig. 7D). In the probe trial, PNS+RU486 group showed improved spatial memory retention as indicated by the PNS+RU486 group spent more time in the target quad-rant and crossed the platform area more times (Fig. 7E, F). In the NOR test, there was no significant difference in the preference index between the four groups during the train-ing phase (Fig. 7G), indicating that these objects did not affect the exploratory behavior of the four groups. In the testing phase, the recognition index of the PNS+RU486 group was higher than PNS+VEH (Fig. 7H). In the Y-maze test, the percentage of spontaneous alternations was sig-nificantly higher in the PNS+RU486 group compared to the PNS+VEH group (Fig. 7I). In conclusion, 3 weeks of RU486 treatment significantly improved cognitive impair-ment in PNS mice.

Next, we investigated the effects of RU486 treatment on GR/Ahi1-WDR68-DYRK1A signaling and synaptic plas-ticity. It was found that the expression of Ahi1, GR and WDR68 was increased while the expression of DYRK1A was decreased in the hippocampus of the PNS+RU486 group compared to the PNS+VEH group (Fig. 8A). Spine density in CA1 and DG was significantly lower in the PNS+VEH group compared to the CON+VEH group, and after 3 weeks of treatment with RU486, spine density was significantly higher in the PNS+RU486 group compared to the PNS+VEH group (Fig. 8B–D). The above results indi-cate that RU486 increases the expression of Ahi1 and GR and ameliorates synaptic plasticity and cognitive impair-ment in prenatally stressed offspring, further confirming that GR/Ahi1 regulates WDR68-DYRK1A binding and medi-ates cognitive impairment in prenatally stressed offspring. Based on our findings, we propose that prenatal stress leads
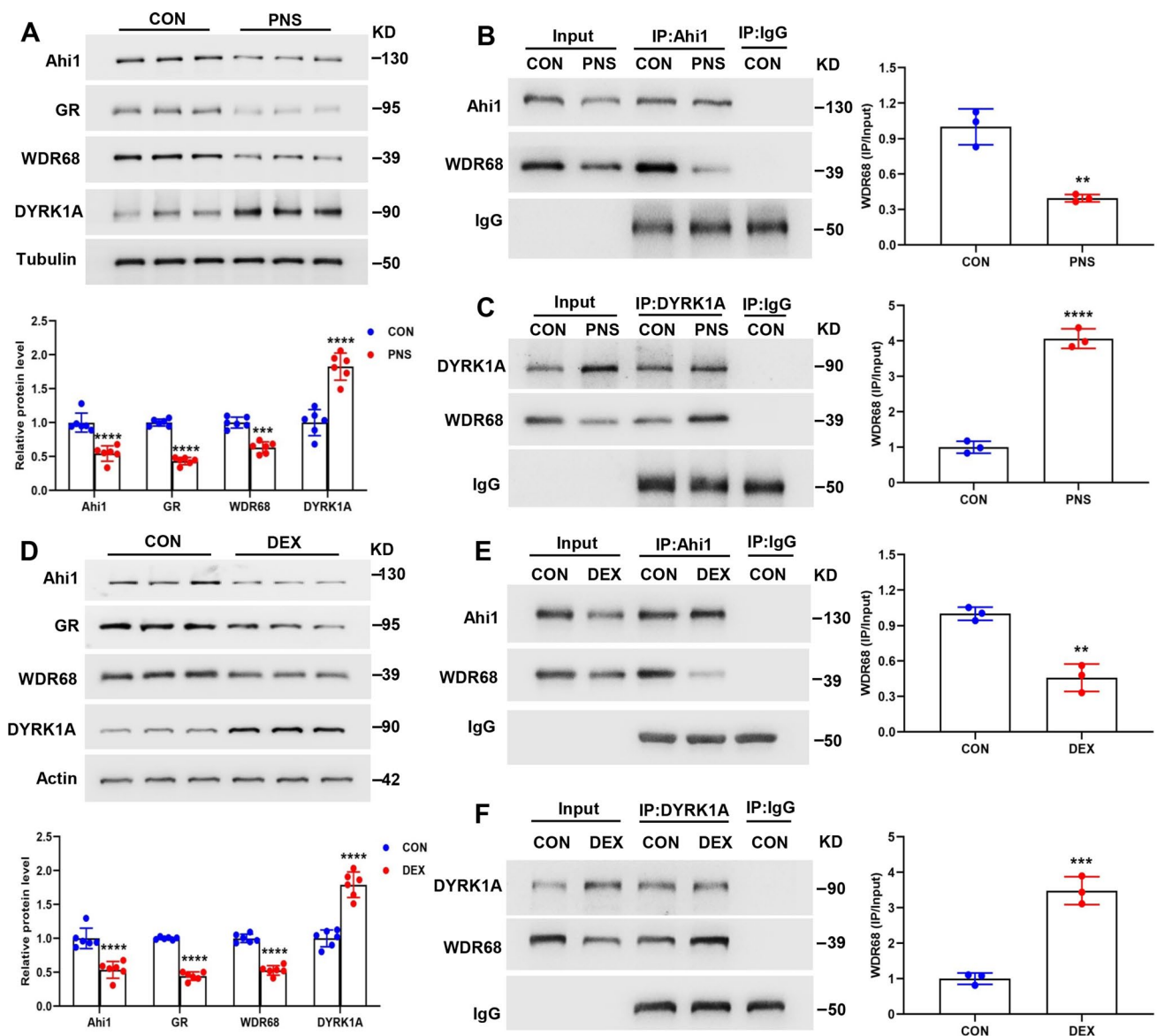
Fig. 6 Prenatal stress alters GR/Ahi1-WDR68-DYRK1A signaling, resulting in decreased binding of Ahi1 to WDR68 and increased binding of WDR68 to DYRK1A. Western blotting demonstrated decreased expression of Ahi1, GR, and WDR68 and increased expression of DYRK1A in the hippocampus of the PNS group. N=6 mice (**A**). Hippocampal tissues from PNS and CON mice were collected and immunoprecipitated with Ahi1 antibody, and Western blotting showed decreased binding between Ahi1 and WDR68. N=3 mice (**B**). Hippocampal tissue from PNS and CON mice was collected and immunoprecipitated with DYRK1A antibody, and Western blotting revealed increased binding between DYRK1A and WDR68.

N=3 mice (**C**). PC12 cells were treated with Dex (20 μM) for 72 h and Western blotting results showed a decrease in the expression of Ahi1, GR and WDR68 and an increase in the expression of DYRK1A in Dex-treated PC12 cells. N=6 cell samples (**D**). PC12 cells from DEX and CON groups were collected and immunoprecipitated with Ahi1 antibody, and Western blotting showed reduced binding between Ahi1 and WDR68. n=3 cell samples (**E**). PC12 cells from DEX and CON groups were collected and immunoprecipitated with DYRK1A antibody and Western blotting showed increased binding between DYRK1A and WDR68. n=3 cell samples (**F**). **$P<0.01$; ***$P<0.001$; ****$P<0.0001$

to an increase in GR nuclear translocation and degradation of Ahi1, and the reduction of Ahi1 leads to a decrease in binding of Ahi1 to WDR68, which promotes the binding of WDR68 and DYRK1A, and an increase in DYRK1A level, which modulates prenatal stress-induced cognitive impairment (Fig. 8E).

Discussion

Accumulating evidence has demonstrated that prenatal stress is associated with an increased risk of emotional, behavioral, and cognitive problems in offspring, and these symptoms include anxiety and depression, ADHD,
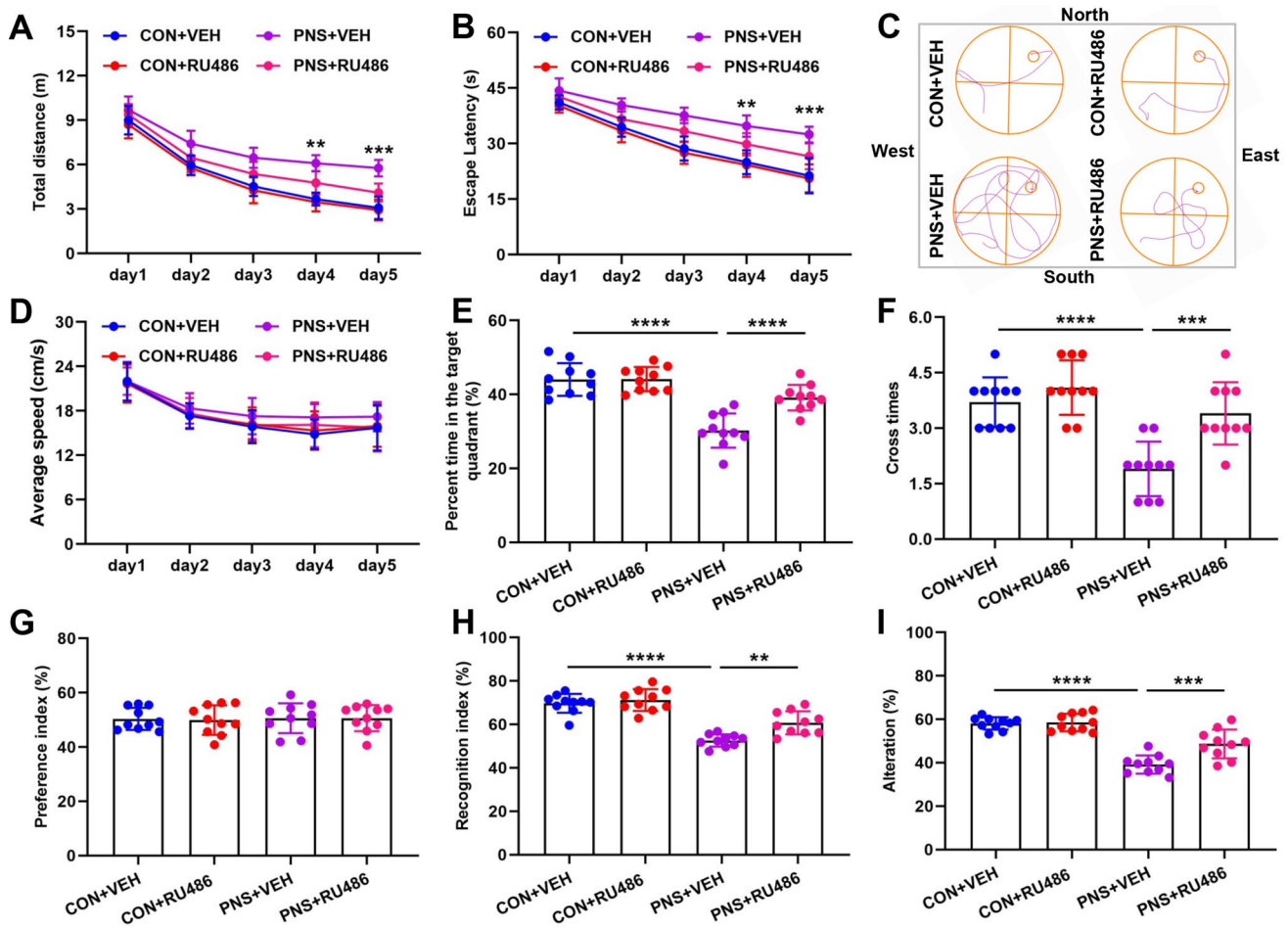
Fig. 7 RU486 ameliorates cognitive impairment in prenatally stressed offspring. Prenatal stress mice and control mice were divided into four groups: CON+VEH, CON+RU486, PNS+VEH, and PNS+RU486. After 3 weeks of treatment with RU486 (20 mg/kg) or vehicle, behavioral tests were performed in four groups. In the MWM test, movement distance (**A**), escape latency (**B**), a representa-tive image of the swim path (**C**), speed of movement (**D**), time spent in the target quadrant (**E**), and number of times crossing the platform area (**F**) were recorded. n = 10 mice. In the NOR test, preference index (**G**) and recognition index (**H**) were recorded. N = 10 mice. In the Y-maze test, the percentage of spontaneous alternations was recorded. N = 10 mice (**I**). **$P < 0.01$; ***$P < 0.001$; ****$P < 0.0001$

and cognitive impairment [63]. The prenatal period is an extremely important and sensitive phase of life, and exposure to stressful events during pregnancy may lead to maternal release of stress hormones such as cortisol in humans and corticosterone in rodents [72]. Excess gluco-corticoids induced by prenatal stress cross the placenta, impairing fetal HPA development and altering the balance of HPA axis activity in offspring [7]. The hippocampus is the brain region with the highest expression of GR, and activation of hippocampal GR negatively feedback regu-lates HPA axis activity by inhibiting the expression of corticotropin-releasing factor or hormone (CRF or CRH) in the paraventricular nucleus (PVN) region [7, 73]. Accu-mulating evidence suggests that reduced expression and impaired function of GR are also associated with elevated offspring HPA axis reactivity induced by prenatal stress [9, 74]. Our previous studies revealed that Ahi1 interacts with GR and regulates nuclear translocation of GR, which is involved in GR-mediated stress response [27].

Ahi1 is abundantly expressed in neurons, functions in intracellular signaling and trafficking, and plays an impor-tant role in early brain development [30, 38, 75]. AHI1 is associated with developmental brain disorders such as Joubert syndrome, which is accompanied by abnormali-ties in brain development as well as cognitive and behav-ioral impairments [22, 76] and neuropsychiatric disorders such as autism, depression and schizophrenia [22, 77–79]. Our previous study found that Ahi1$^{-/-}$ mice exhibit typical depression-like behaviors and that AHI1 deficiency desta-bilizes GR, which regulates the expression of depression-related genes in the brain [23–25, 27, 80]. Studies have demonstrated reduced AHI1 expression in serum of patients with AD and the brains of 3xTg-AD mice, suggesting that AHI1 may be associated with cognition [28, 29]. In this
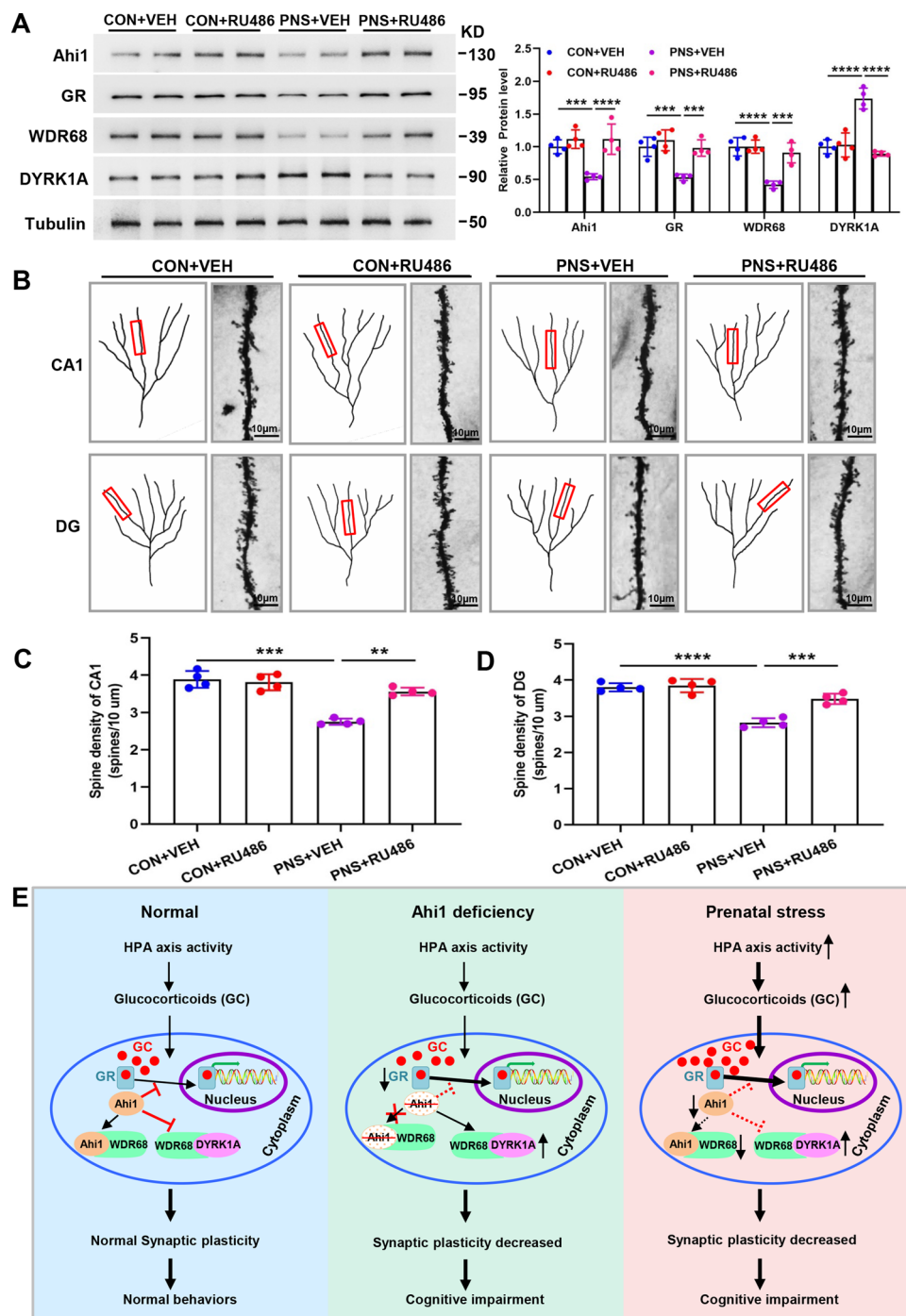
Fig. 8 RU486 increases hippocampal GR and Ahi1 levels and improves synaptic plasticity in prenatally stressed offspring. After RU486 or vehicle treatment of PNS and CON mice for 3 weeks, hippocampal tissues of the mice were collected, and Western blotting showed that the expression of Ahi1, GR, and WDR68 was increased in the hippocampus of the PNS+RU486 group compared to the PNS+VEH group, while the expression of DYRK1A was decreased. N = 6 mice (**A**). Representative micrographs of dendritic spines in the four groups of mice (**B**). Spine densities of DG and CA1 in the hippocampus of four groups were analyzed. N = 4 mice (**C**, **D**). Proposed diagram of Ahi1/GR signaling regulating WDR68-DYRK1A binding and mediating cognitive impairment. Under normal conditions, glucocorticoids (GC) bind to the GR and enter the nucleus. Ahi1 and GR stabilize each other, inhibit GR nuclear translocation and Ahi1 degradation, promote Ahi1 and WDR68 binding, and inhibit DYRK1A and WDR68 binding. When Ahi1 is absent, it promotes GR nuclear translocation, facilitates DYRK1A and WDR68 binding, and leads to elevated DYRK1A, reduced synaptic plasticity, and demonstrated cognitive impairment. Prenatal stress leads to hyperactivity of the HPA axis promoting release of GC, leading to GR nuclear translocation and degradation of Ahi1, inhibiting Ahi1 and WDR68 binding, and promoting DYRK1A and WDR68 binding, leading to elevated DYRK1A, reduced synaptic plasticity, and cognitive impairment in offspring (**E**). Scale bar = 10 µm. **$P < 0.01$; ***$P < 0.001$; ****$P < 0.0001$

study, we found that Ahi1$^{-/-}$ mice exhibit typical cognitive impairment (Fig. 1) and reduced synaptic plasticity (Fig. 2). Interestingly, we found that prenatal stress resulted in reduced expression of Ahi1 and GR in the hippocampus of the offspring (Fig. 6A) and showed cognitive impairment (Fig. 5D–L). Further studies revealed that elevated serum corticosterone levels in PNS mice (Fig. 5C) promoted GR nuclear translocation (Supplementary Fig. 5), and nuclear translocation of GR reduced the stability and level of Ahi1. Conversely, the reduction of Ahi1 promoted nuclear translocation of GR.

Ahi1 and Hap1 are able to form a stable complex regulating early brain development [30], and Hap1 interacts with the craniofacial development-associated protein WDR68 [31]. In this study, we found that Ahi1 also binds WDR68 (Fig. 3A–C) and regulates WDR68 expression. WDR68 protein expression was decreased in Ahi1$^{-/-}$ mice and PC12 cells with knockdown of Ahi1, while WDR68 protein expression was increased in PC12 cells overexpressing Ahi1 (Fig. 3E–G). In addition, we found that Ahi1 was able to stabilize WDR68 and inhibit its degradation as indicated by knockdown of Ahi1 in PC12 cells significantly shortened the half-life of WDR68, and overexpression of Ahi1 significantly lengthened the half-life of WDR68 (Supplementary Fig. 2) Consistently, WDR68 ubiquitination degradation was increased in Ahi1$^{-/-}$ mice and decreased in PC12 cells overexpressing Ahi1 (Fig. 3H, I). Previous report has shown that overexpression of Hap1 (but not Ahi1) in HEK239 cells increased WDR68 protein levels [31]. However, the study selected the HEK293 cell line (a type of cell that does not express Hap1 but expresses Ahi1) [31, 81], so the role of endogenous Ahi1 was not ruled out. To further investigate whether Ahi1 regulates WDR68 expression through Hap1, we chose the Hela cell line (a cell line that expresses neither Ahi1 nor Hap1), and found that transfecting Ahi1 and Hap1 together into Hela cells increased WDR68 expression (Supplementary Fig. 7). Therefore, we hypothesized that Ahi1 and Hap1 form a complex to co-regulate WDR68 expression, and that the lack of either Ahi1 or Hap1 does not function to regulate WDR68 expression.

DYRK1A is a highly conserved protein kinase belonging to the dual-specificity tyrosine phosphorylation-regulated kinase (DYRK) family that interacts with WDR68 [82, 83]. DYRK1A has multiple functions in central nervous system (CNS) development, including neurogenesis, neuronal differentiation, proliferation, cell death, and synaptic plasticity [84]. DYRK1A is closely related to AD and DS, and inhibition of its expression ameliorates cognitive impairment in animal models of AD and DS [36, 37]. In the present study, we found that Ahi1 deficiency elevated DYRK1A level, while increased Ahi1 inhibited DYRK1A level (Fig. 4B–D). In addition, DYRK1A and Ahi1 may compete for WDR68 binding, and WDR68

binding may be important for DYRK1A stability as indicated by Ahi1$^{-/-}$ mice exhibited increased DYRK1A and WDR68 binding (Fig. 4E), whereas Ahi1 overexpressing PC12 cells had decreased DYRK1A and WDR68 binding (Fig. 4F), and DYRK1A overexpressing PC12 cells had decreased Ahi1 and WDR68 binding (Fig. 4G). Consistently, Ahi1 and WDR68 binding and WDR68 expression were also reduced in PNS mice and Dex-treated PC12 cells, while DYRK1A and WDR68 binding and DYRK1A levels were increased (Fig. 6). Thus, GR/Ahi1 may regulate WDR68-DYRK1A binding and mediate cognitive deficits in prenatally stressed offspring. To further confirm the role of GR/Ahi1 in modulating cognitive deficits in prenatally stressed offspring, we administered the GR antagonist RU486 to PNS and CON mice for 3 weeks, and found that RU486 significantly ameliorated cognitive impairments in PNS mice (Fig. 7), and further investigations revealed that RU486 increased the levels of Ahi1, GR and WDR68, decreased the level of DYRK1A, and improved synaptic plasticity in PNS mice (Fig. 8). Thus, this study further confirms that GR/Ahi1 regulation of WDR68-DYRK1A binding plays a crucial role in mediating cognitive deficits in prenatally stressed offspring.

Conclusions

In this study, we demonstrate that Ahi1 and DYRK1A compete for WDR68 binding and Ahi1$^{-/-}$ mice exhibit cognitive impairment. GR/Ahi1 regulates WDR68-DYRK1A binding and mediates cognitive impairment in prenatally stressed offspring. Thus, GR/Ahi1 may be a therapeutic target for treating stress-mediated cognitive impairment in offspring.

Declarations

Conflict of interest The authors declare that they have no potential conflicts of interest.

Ethical approval All experiments were performed strictly follow the guidelines of the University Committee on Animal Care of Soochow University.

Consent for publication All the authors read and approved the submission and final publication.

References

1. Barker DJ, Winter PD, Osmond C et al (1989) Weight in infancy and death from ischaemic heart disease. Lancet 2(8663):577–580. https://doi.org/10.1016/s0140-6736(89)90710-1

2. Wang B, Zeng H, Liu J et al (2021) Effects of prenatal hypoxia on nervous system development and related diseases. Front Neurosci 15:755554. https://doi.org/10.3389/fnins.2021.755554

3. Gluckman PD, Hanson MA, Cooper C et al (2008) Effect of in utero and early-life conditions on adult health and disease. N Engl J Med 359(1):61–73. https://doi.org/10.1056/NEJMra0708473

4. Pallares ME, Antonelli MC (2017) Prenatal stress and neurodevelopmental plasticity: relevance to psychopathology. Adv Exp Med Biol 1015:117–129. https://doi.org/10.1007/978-3-319-62817-2_7

5. Moura CA, Oliveira MC, Costa LF et al (2020) Prenatal restraint stress impairs recognition memory in adult male and female offspring. Acta Neuropsychiatr. https://doi.org/10.1017/neu.2020.3

6. Son GH, Geum D, Chung S et al (2006) Maternal stress produces learning deficits associated with impairment of NMDA receptor-mediated synaptic plasticity. J Neurosci 26(12):3309–3318. https://doi.org/10.1523/JNEUROSCI.3850-05.2006

7. Liu MY, Wei LL, Zhu XH et al (2023) Prenatal stress modulates HPA axis homeostasis of offspring through dentate TERT independently of glucocorticoids receptor. Mol Psychiatry 28(3):1383–1395. https://doi.org/10.1038/s41380-022-01898-9

8. Pariante CM, Lightman SL (2008) The HPA axis in major depression: classical theories and new developments. Trends Neurosci 31(9):464–468. https://doi.org/10.1016/j.tins.2008.06.006

9. Barbazanges A, Piazza PV, Le Moal M et al (1996) Maternal glucocorticoid secretion mediates long-term effects of prenatal stress. J Neurosci 16(12):3943–3949. https://doi.org/10.1523/JNEUROSCI.16-12-03943.1996

10. Cottrell EC, Seckl JR (2009) Prenatal stress, glucocorticoids and the programming of adult disease. Front Behav Neurosci 3:19. https://doi.org/10.3389/neuro.08.019.2009

11. Luft C, Levices IP, da Costa MS et al (2021) Effects of running before pregnancy on long-term memory and hippocampal alterations induced by prenatal stress. Neurosci Lett 746:135659. https://doi.org/10.1016/j.neulet.2021.135659

12. Wang Q, Van Heerikhuize J, Aronica E et al (2013) Glucocorticoid receptor protein expression in human hippocampus; stability with age. Neurobiol Aging 34(6):1662–1673. https://doi.org/10.1016/j.neurobiolaging.2012.11.019

13. Knierim JJ (2015) The hippocampus. Curr Biol 25(23):R1116–R1121. https://doi.org/10.1016/j.cub.2015.10.049

14. Phillips LJ, McGorry PD, Garner B et al (2006) Stress, the hippocampus and the hypothalamic–pituitary–adrenal axis: implications for the development of psychotic disorders. Aust N Z J Psychiatry 40(9):725–741. https://doi.org/10.1080/j.1440-1614.2006.01877.x

15. Scheinost D, Spann MN, McDonough L et al (2020) Associations between different dimensions of prenatal distress, neonatal hippocampal connectivity, and infant memory. Neuropsychopharmacology 45(8):1272–1279. https://doi.org/10.1038/s41386-020-0677-0

16. Shang Y, Chen R, Li F et al (2021) Prenatal stress impairs memory function in the early development of male-offspring associated with the gaba function. Physiol Behav 228:113184. https://doi.org/10.1016/j.physbeh.2020.113184

17. Martinez-Tellez RI, Hernandez-Torres E, Gamboa C et al (2009) Prenatal stress alters spine density and dendritic length of nucleus accumbens and hippocampus neurons in rat offspring. Synapse 63(9):794–804. https://doi.org/10.1002/syn.20664

18. Jenkins S, Harker A, Gibb R (2022) Maternal stress prior to conception impairs memory and decreases right dorsal hippocampal volume and basilar spine density in the prefrontal cortex of adult male offspring. Behav Brain Res 416:113543. https://doi.org/10.1016/j.bbr.2021.113543

19. Barzegar M, Sajjadi FS, Talaei SA et al (2015) Prenatal exposure to noise stress: anxiety, impaired spatial memory, and deteriorated hippocampal plasticity in postnatal life. Hippocampus 25(2):187–196. https://doi.org/10.1002/hipo.22363

20. Li YJ, Yang LP, Hou JL et al (2020) Prenatal Stress Impairs Postnatal Learning and Memory Development via Disturbance of the cGMP-PKG Pathway and Oxidative Phosphorylation in the Hippocampus of Rats. Front Mol Neurosci 13:158. https://doi.org/10.3389/fnmol.2020.00158

21. Zhang H, Shang Y, Xiao X et al (2017) Prenatal stress-induced impairments of cognitive flexibility and bidirectional synaptic plasticity are possibly associated with autophagy in adolescent male-offspring. Exp Neurol 298(Pt A):68–78. https://doi.org/10.1016/j.expneurol.2017.09.001

22. Ferland RJ, Eyaid W, Collura RV et al (2004) Abnormal cerebellar development and axonal decussation due to mutations in AHI1 in Joubert syndrome. Nat Genet 36(9):1008–1013. https://doi.org/10.1038/ng1419

23. Xu X, Yang H, Lin YF et al (2010) Neuronal Abelson helper integration site-1 (Ahi1) deficiency in mice alters TrkB signaling with a depressive phenotype. Proc Natl Acad Sci USA 107(44):19126–19131. https://doi.org/10.1073/pnas.1013032107

24. Wang B, Shi H, Ren L et al (2022) Ahi1 regulates serotonin production by the GR/ERbeta/TPH2 pathway involving sexual differences in depressive behaviors. Cell Commun Signal 20(1):74. https://doi.org/10.1186/s12964-022-00894-4

25. Wang B, Shi H, Yang B et al (2023) The mitochondrial Ahi1/GR participates the regulation on mtDNA copy numbers and brain ATP levels and modulates depressive behaviors in mice. Cell Commun Signal 21(1):21. https://doi.org/10.1186/s12964-022-01034-8

26. Ren L, Qian X, Zhai L et al (2014) Loss of Ahi1 impairs neurotransmitter release and causes depressive behaviors in mice. PLoS ONE 9(4):e93640. https://doi.org/10.1371/journal.pone.0093640

27. Wang B, Xin N, Qian X et al (2021) Ahi1 regulates the nuclear translocation of glucocorticoid receptor to modulate stress response. Transl Psychiatry 11(1):188. https://doi.org/10.1038/s41398-021-01305-x

28. Ting LL, Lu HT, Yen SF et al (2019) Expression of AHI1 rescues amyloidogenic pathology in Alzheimer's disease model cells. Mol Neurobiol 56(11):7572–7582. https://doi.org/10.1007/s12035-019-1587-1

29. Sheu JJ, Yang LY, Sanotra MR et al (2020) Reduction of AHI1 in the serum of Taiwanese with probable Alzheimer's disease. Clin Biochem 76:24–30. https://doi.org/10.1016/j.clinbiochem.2019.11.011

30. Sheng G, Xu X, Lin YF et al (2008) Huntingtin-associated protein 1 interacts with Ahi1 to regulate cerebellar and brainstem

development in mice. J Clin Invest 118(8):2785–2795. https://doi.org/10.1172/JCI35339

31. Xiang J, Yang S, Xin N et al (2017) DYRK1A regulates Hap1-Dcaf7/WDR68 binding with implication for delayed growth in Down syndrome. Proc Natl Acad Sci USA 114(7):E1224–E1233. https://doi.org/10.1073/pnas.1614893114

32. Ryu YS, Park SY, Jung MS et al (2010) Dyrk1A-mediated phosphorylation of Presenilin 1: a functional link between Down syndrome and Alzheimer's disease. J Neurochem 115(3):574–584. https://doi.org/10.1111/j.1471-4159.2010.06769.x

33. Ferrer I, Barrachina M, Puig B et al (2005) Constitutive Dyrk1A is abnormally expressed in Alzheimer disease, Down syndrome, Pick disease, and related transgenic models. Neurobiol Dis 20(2):392–400. https://doi.org/10.1016/j.nbd.2005.03.020

34. Ryoo SR, Cho HJ, Lee HW et al (2008) Dual-specificity tyrosine(Y)-phosphorylation regulated kinase 1A-mediated phosphorylation of amyloid precursor protein: evidence for a functional link between Down syndrome and Alzheimer's disease. J Neurochem 104(5):1333–1344. https://doi.org/10.1111/j.1471-4159.2007.05075.x

35. Ahn KJ, Jeong HK, Choi HS et al (2006) DYRK1A BAC transgenic mice show altered synaptic plasticity with learning and memory defects. Neurobiol Dis 22(3):463–472. https://doi.org/10.1016/j.nbd.2005.12.006

36. Altafaj X, Martin ED, Ortiz-Abalia J et al (2013) Normalization of Dyrk1A expression by AAV2/1-shDyrk1A attenuates hippocampal-dependent defects in the Ts65Dn mouse model of Down syndrome. Neurobiol Dis 52:117–127. https://doi.org/10.1016/j.nbd.2012.11.017

37. Velazquez R, Meechoovet B, Ow A et al (2019) Chronic Dyrk1 inhibition delays the onset of AD-like pathology in 3xTg-AD mice. Mol Neurobiol 56(12):8364–8375. https://doi.org/10.1007/s12035-019-01684-9

38. Weng L, Lin YF, Li AL et al (2013) Loss of Ahi1 affects early development by impairing BM88/Cend1-mediated neuronal differentiation. J Neurosci 33(19):8172–8184. https://doi.org/10.1523/JNEUROSCI.0119-13.2013

39. Liston C, Gan WB (2011) Glucocorticoids are critical regulators of dendritic spine development and plasticity in vivo. Proc Natl Acad Sci USA 108(38):16074–16079. https://doi.org/10.1073/pnas.1110444108

40. de Pablos RM, Villaran RF, Arguelles S et al (2006) Stress increases vulnerability to inflammation in the rat prefrontal cortex. J Neurosci 26(21):5709–5719. https://doi.org/10.1523/JNEUROSCI.0802-06.2006

41. Lu MH, Zhao XY, Xu DE et al (2020) Transplantation of GABAergic interneuron progenitor attenuates cognitive deficits of Alzheimer's disease model mice. J Alzheimers Dis 75(1):245–260. https://doi.org/10.3233/JAD-200010

42. Yuan DJ, Yang G, Wu W et al (2022) Reducing Nav1.6 expression attenuates the pathogenesis of Alzheimer's disease by suppressing BACE1 transcription. Aging Cell 21(5):e13593. https://doi.org/10.1111/acel.13593

43. Lu MH, Ji WL, Chen H et al (2021) Intranasal transplantation of human neural stem cells ameliorates Alzheimer's disease-like pathology in a mouse model. Front Aging Neurosci 13:650103. https://doi.org/10.3389/fnagi.2021.650103

44. Su Q, Li T, He PF et al (2021) Trichostatin A ameliorates Alzheimer's disease-related pathology and cognitive deficits by increasing albumin expression and Abeta clearance in APP/PS1 mice. Alzheimers Res Ther 13(1):7. https://doi.org/10.1186/s13195-020-00746-8

45. Jiang R, Wu XF, Wang B et al (2020) Reduction of NgR in perforant path decreases amyloid-beta peptide production and ameliorates synaptic and cognitive deficits in APP/PS1 mice. Alzheimers Res Ther 12(1):47. https://doi.org/10.1186/s13195-020-00616-3

46. Gao JM, Zhang X, Shu GT et al (2022) Trilobatin rescues cognitive impairment of Alzheimer's disease by targeting HMGB1 through mediating SIRT3/SOD2 signaling pathway. Acta Pharmacol Sin 43(10):2482–2494. https://doi.org/10.1038/s41401-022-00888-5

47. Wang B, Zheng Y, Shi H et al (2017) Zfp462 deficiency causes anxiety-like behaviors with excessive self-grooming in mice. Genes Brain Behav 16(2):296–307. https://doi.org/10.1111/gbb.12339

48. Crawley J, Goodwin FK (1980) Preliminary report of a simple animal behavior model for the anxiolytic effects of benzodiazepines. Pharmacol Biochem Behav 13(2):167–170. https://doi.org/10.1016/0091-3057(80)90067-2

49. Bourin M, Hascoet M (2003) The mouse light/dark box test. Eur J Pharmacol 463(1–3):55–65. https://doi.org/10.1016/s0014-2999(03)01274-3

50. Gao Q, Gao Y, Song H et al (2016) Cipadesin A, a bioactive ingredient of *Xylocarpus granatum*, produces antidepressant-like effects in adult mice. Neurosci Lett 633:33–39. https://doi.org/10.1016/j.neulet.2016.08.062

51. Wang B, Zhang Y, Dong H et al (2018) Loss of Tctn3 causes neuronal apoptosis and neural tube defects in mice. Cell Death Dis 9(5):520. https://doi.org/10.1038/s41419-018-0563-4

52. Zhao W, Xu Z, Cao J et al (2019) Elamipretide (SS-31) improves mitochondrial dysfunction, synaptic and memory impairment induced by lipopolysaccharide in mice. J Neuroinflamm 16(1):230. https://doi.org/10.1186/s12974-019-1627-9

53. Cheyne JE, Montgomery JM (2020) The cellular and molecular basis of in vivo synaptic plasticity in rodents. Am J Physiol Cell Physiol 318(6):C1264–C1283. https://doi.org/10.1152/ajpcell.00416.2019

54. Fan M, Liu Y, Shang Y et al (2022) JADE2 is essential for hippocampal synaptic plasticity and cognitive functions in mice. Biol Psychiatry 92(10):800–814. https://doi.org/10.1016/j.biopsych.2022.05.021

55. Kandel ER, Dudai Y, Mayford MR (2014) The molecular and systems biology of memory. Cell 157(1):163–186. https://doi.org/10.1016/j.cell.2014.03.001

56. Davies DA, Adlimoghaddam A, Albensi BC (2021) Role of Nrf2 in synaptic plasticity and memory in Alzheimer's disease. Cells. https://doi.org/10.3390/cells10081884

57. Zhang MY, Zheng CY, Zou MM et al (2014) Lamotrigine attenuates deficits in synaptic plasticity and accumulation of amyloid plaques in APP/PS1 transgenic mice. Neurobiol Aging 35(12):2713–2725. https://doi.org/10.1016/j.neurobiolaging.2014.06.009

58. Miyata Y, Shibata T, Aoshima M et al (2014) The molecular chaperone TRiC/CCT binds to the Trp-Asp 40 (WD40) repeat protein WDR68 and promotes its folding, protein kinase DYRK1A binding, and nuclear accumulation. J Biol Chem 289(48):33320–33332. https://doi.org/10.1074/jbc.M114.586115

59. Alvarado E, Yousefelahiyeh M, Alvarado G et al (2016) Wdr68 mediates dorsal and ventral patterning events for craniofacial development. PLoS ONE 11(11):e0166984. https://doi.org/10.1371/journal.pone.0166984

60. Murphy MO, Cohn DM, Loria AS (2017) Developmental origins of cardiovascular disease: impact of early life stress in humans and rodents. Neurosci Biobehav Rev 74(Pt B):453–465. https://doi.org/10.1016/j.neubiorev.2016.07.018

61. Chen K, Sun D, Qu S et al (2019) Prenatal cold exposure causes hypertension in offspring by hyperactivity of the sympathetic nervous system. Clin Sci (Lond) 133(9):1097–1113. https://doi.org/10.1042/CS20190254

62. Jiang X, Ma H, Wang Y et al (2013) Early life factors and type 2 diabetes mellitus. J Diabetes Res 2013:485082. https://doi.org/10.1155/2013/485082

63. Lautarescu A, Craig MC, Glover V (2020) Prenatal stress: effects on fetal and child brain development. Int Rev Neurobiol 150:17–40. https://doi.org/10.1016/bs.irn.2019.11.002

64. Cao K, Zheng A, Xu J et al (2014) AMPK activation prevents prenatal stress-induced cognitive impairment: modulation of mitochondrial content and oxidative stress. Free Radic Biol Med 75:156–166. https://doi.org/10.1016/j.freeradbiomed.2014.07.029

65. Eberle C, Fasig T, Bruseke F et al (2021) Impact of maternal prenatal stress by glucocorticoids on metabolic and cardiovascular outcomes in their offspring: a systematic scoping review. PLoS ONE 16(1):e0245386. https://doi.org/10.1371/journal.pone.0245386

66. Harris A, Seckl J (2011) Glucocorticoids, prenatal stress and the programming of disease. Horm Behav 59(3):279–289. https://doi.org/10.1016/j.yhbeh.2010.06.007

67. Buitelaar JK, Huizink AC, Mulder EJ et al (2003) Prenatal stress and cognitive development and temperament in infants. Neurobiol Aging 24(Suppl 1):S53–S60; discussion S67–S68. https://doi.org/10.1016/s0197-4580(03)00050-2

68. Lemaire V, Koehl M, Le Moal M et al (2000) Prenatal stress produces learning deficits associated with an inhibition of neurogenesis in the hippocampus. Proc Natl Acad Sci USA 97(20):11032–11037. https://doi.org/10.1073/pnas.97.20.11032

69. Zheng Y, Zhang YM, Tang ZS et al (2021) Spatial learning and memory deficits induced by prenatal glucocorticoid exposure depend on hippocampal CRHR1 and CXCL5 signaling in rats. J Neuroinflamm 18(1):85. https://doi.org/10.1186/s12974-021-02129-8

70. Belanoff JK, Jurik J, Schatzberg LD et al (2002) Slowing the progression of cognitive decline in Alzheimer's disease using mifepristone. J Mol Neurosci 19(1–2):201–206. https://doi.org/10.1007/s12031-002-0033-3

71. Dhikav V, Anand KS (2007) Glucocorticoids may initiate Alzheimer's disease: a potential therapeutic role for mifepristone (RU-486). Med Hypotheses 68(5):1088–1092. https://doi.org/10.1016/j.mehy.2006.09.038

72. Creutzberg KC, Sanson A, Viola TW et al (2021) Long-lasting effects of prenatal stress on HPA axis and inflammation: a systematic review and multilevel meta-analysis in rodent studies. Neurosci Biobehav Rev 127:270–283. https://doi.org/10.1016/j.neubiorev.2021.04.032

73. Jankord R, Herman JP (2008) Limbic regulation of hypothalamo-pituitary-adrenocortical function during acute and chronic stress. Ann N Y Acad Sci 1148:64–73. https://doi.org/10.1196/annals.1410.012

74. Palma-Gudiel H, Cordova-Palomera A, Eixarch E et al (2015) Maternal psychosocial stress during pregnancy alters the epigenetic signature of the glucocorticoid receptor gene promoter in their offspring: a meta-analysis. Epigenetics 10(10):893–902. https://doi.org/10.1080/15592294.2015.1088630

75. Jiang X, Hanna Z, Kaouass M et al (2002) Ahi-1, a novel gene encoding a modular protein with WD40-repeat and SH3 domains, is targeted by the Ahi-1 and Mis-2 provirus integrations. J Virol 76(18):9046–9059. https://doi.org/10.1128/jvi.76.18.9046-9059.2002

76. Dixon-Salazar T, Silhavy JL, Marsh SE et al (2004) Mutations in the AHI1 gene, encoding jouberin, cause Joubert syndrome with cortical polymicrogyria. Am J Hum Genet 75(6):979–987. https://doi.org/10.1086/425985

77. Alvarez Retuerto AI, Cantor RM, Gleeson JG et al (2008) Association of common variants in the Joubert syndrome gene (AHI1) with autism. Hum Mol Genet 17(24):3887–3896. https://doi.org/10.1093/hmg/ddn291

78. Porcelli S, Pae CU, Han C et al (2014) Abelson helper integration site-1 gene variants on major depressive disorder and bipolar disorder. Psychiatry Investig 11(4):481–486. https://doi.org/10.4306/pi.2014.11.4.481

79. Rivero O, Reif A, Sanjuan J et al (2010) Impact of the AHI1 gene on the vulnerability to schizophrenia: a case-control association study. PLoS ONE 5(8):e12254. https://doi.org/10.1371/journal.pone.0012254

80. Zhang HG, Wang B, Yang Y et al (2022) Depression compromises antiviral innate immunity via the AVP-AHI1-Tyk2 axis. Cell Res 32(10):897–913. https://doi.org/10.1038/s41422-022-00689-9

81. Eley L, Gabrielides C, Adams M et al (2008) Jouberin localizes to collecting ducts and interacts with nephrocystin-1. Kidney Int 74(9):1139–1149. https://doi.org/10.1038/ki.2008.377

82. Galceran J, de Graaf K, Tejedor FJ et al (2003) The MNB/DYRK1A protein kinase: genetic and biochemical properties. J Neural Transm Suppl 67:139–148. https://doi.org/10.1007/978-3-7091-6721-2_12

83. Miyata Y (1813) Nishida E (2011) DYRK1A binds to an evolutionarily conserved WD40-repeat protein WDR68 and induces its nuclear translocation. Biochim Biophys Acta 10:1728–1739. https://doi.org/10.1016/j.bbamcr.2011.06.023

84. Tejedor FJ, Hammerle B (2011) MNB/DYRK1A as a multiple regulator of neuronal development. FEBS J 278(2):223–235. https://doi.org/10.1111/j.1742-4658.2010.07954.x